

# Decay of standard model-like Higgs boson $h \rightarrow \mu\tau$ in a 3-3-1 model with inverse seesaw neutrino masses

T. Phong Nguyen,<sup>1,\*</sup> T.Thuy Le,<sup>2,†</sup> T.T. Hong,<sup>3,4,‡</sup> and L.T. Hue<sup>§5,6,¶</sup>

<sup>1</sup>*Department of Physics, Can Tho University, 3/2 Street, Can Tho, Vietnam*

<sup>2</sup>*People's security high school II, Ap Bac street, My Tho, Tien Giang, Viet Nam*

<sup>3</sup>*Department of Physics, An Giang University,*

*Ung Van Khiem Street, Long Xuyen, An Giang, Vietnam*

<sup>4</sup>*Department of Physics, Hanoi Pedagogical University 2, Phuc Yen, Vinh Phuc, Vietnam*

<sup>5</sup>*Institute for Research and Development,*

*Duy Tan University, Da Nang City, Vietnam*

<sup>6</sup>*Institute of Physics, Vietnam Academy of Science and Technology,*

*10 Dao Tan, Ba Dinh, Hanoi, Vietnam*

## Abstract

By adding new gauge singlets of neutral leptons, improved versions of the 3-3-1 models with right-handed neutrinos have been introduced recently to explain recent experimental data of neutrino oscillation through the inverse seesaw mechanism. We will prove that these models predict promising signals of lepton flavor violating decays of the standard model like-Higgs boson  $h_1^0 \rightarrow \mu\tau, e\tau$ , which are suppressed in the original versions. One-loop contributions to these decay amplitudes are introduced in the unitary gauge. Based on numerical investigation, we find that the branching ratios decays  $h_1^0 \rightarrow \mu\tau, e\tau$  can reach values of  $10^{-5}$  in the regions of the parameter space satisfying the current experimental data of the decay  $\mu \rightarrow e\gamma$ . The value of  $10^{-4}$  appears when Yukawa couplings of leptons are close to the perturbative limit. Interesting properties of these regions of the parameter space are discussed.

PACS numbers: 12.15.Lk, 12.60.-i, 13.15.+g, 14.60.St

---

<sup>§</sup> Corresponding author

<sup>\*</sup>Electronic address: thanhphong@ctu.edu.vn

<sup>†</sup>Electronic address: lethuthuy09a@gmail.com

<sup>‡</sup>Electronic address: tthong@agu.edu.vn

<sup>¶</sup>Electronic address: lthue@iop.vast.ac.vn

## I. INTRODUCTION

Signal of lepton flavor violating decays of the Standard model-like Higgs boson (LFVHD) has been searched at LHC [1] not very long after its discovery at LHC in 2012 [2]. So far, the most stringent limit of the branching ratios (Br) of these decay are  $\text{Br}(h \rightarrow \mu\tau, e\tau) < \mathcal{O}(10^{-3})$ , concerned by CMS collaboration using the collected data at a centre-of-mass energy of 13 TeV. Many studies of the sensitivities of the planned colliders for LFVHD searches predict the possibilities of detection at order of  $10^{-5}$  [3].

In the theoretical side, model-independent studies showed that the LFVHD predicted from models beyond the SM (BSM) are constrained indirectly from other experimental data such as lepton flavor violating decays of charged leptons (cLFV) [4]. Namely, they are affected most strongly on the recent experimental bound of  $\text{Br}(\mu \rightarrow e\gamma)$ . Fortunately, large Brs of decays  $h \rightarrow \mu\tau, e\tau$  are still allowed up to the order of  $10^{-4}$ . Also, LFVHD have been widely investigated in many specific models BSM, where the decay rates were indicated to be close to the upcoming sensitivities of colliders, including non-supersymmetric [5, 6] and supersymmetric version [7]. Among them, models based on the gauge symmetry  $SU(3)_C \times SU(2)_L \times U(1)_X$  (3-3-1) contain rich LFV sources which may result in interesting cLFV phenomenology such as charged lepton decays  $e_i \rightarrow e_j\gamma$  [9–12]. Specially, it was shown that  $\text{Br}(\mu \rightarrow e\gamma)$  is large in these models, hence must be taken into accounts to constrain the parameter space. In addition, such rich LFV resources may give large LFVHD rates as promising signals of new physics.

Although the 3-3-1 models were introduced a long time ago [13, 14], LFVHD has been investigated in the only version with heavy neutral leptons assigned in the third components of lepton (anti-)triplets, where active neutrino masses come from effective operators [35]. The largest values of LFVHD rates were shown to be  $\mathcal{O}(10^{-5})$ , originating from heavy neutrinos and charged Higgs bosons [6]. Recently, improved versions consisting of new neutral lepton singlets have been introduced [9, 15]. They become much more interesting, because they explain successfully the experimental neutrino data through the inverse seesaw (ISS) mechanism. We name them the 331ISS models for short. They predict large cLFV decay rate of  $\mu \rightarrow e\gamma$  corresponding to recent experimental bound. They may also contain dark matter candidates [9, 15]. These properties make them much more attractive than the original versions of 3-3-1 models with right-handed neutrinos (331RHN) [14]. They

predict suppressed lepton flavor violating (LFV) decay rates, because all neutrinos including exotic ones, are extremely light. Furthermore, loop corrections to neutrino mass matrix have to be taken into account to obtain the real active neutrino spectrum [24]. Hence, LFV signals become interesting information to distinguish the 331ISS and 331RHN models. More attraction, a simple inverse seesaw extension of the SM allows large  $\text{Br}(h \rightarrow \mu\tau, e\tau) \sim \mathcal{O}(10^{-5})$ , in the allowed region satisfying  $\text{Br}(\mu \rightarrow e\gamma) < 4.2 \times 10^{-13}$  [18]. Inspired by this, we address some questions in this work: How large  $\text{Br}(h \rightarrow \mu\tau, e\tau)$  do the 331ISS models predict under the experimental constraints of the cLFV decays? Are these Brs larger than the values calculated in the simplest ISS extension of the SM. Because these 331 models contain much more particles contributing to LFV processes through loop corrections, either constructive or destructive correlations among them will affect strongly on the allowed regions of the parameter space satisfying the current bound of the decay rate  $\mu \rightarrow e\gamma$ . The most interesting regions of parameters space will also allow large LFBVD rates, which we will try to look for in this work. Because the discussion on the decay  $h \rightarrow e\tau$  is rather similar to the decay  $h \rightarrow \mu\tau$ , so we just mention on the later.

Our paper is arranged as follows. Sec. II will discuss the necessary ingredients of a 331ISS model for studying LFBVD and how the ISS mechanism works for generating active neutrino parameters consistent with current experimental data. Sec. III will present all couplings needed to determine one-loop amplitudes of the LFBVD of the SM-like Higgs boson. Sec. IV will show important numerical LFBVD results predicted by the 331ISS model. Sec. V remarks our features obtained in this work. Finally, Appendix A lists all analytic formulas expressing private one loop contributions calculated in the unitary gauge.

## II. THE 331ISS MODEL FOR TREE LEVEL NEUTRINO MASSES

### A. The model and neutrino masses from the inverse seesaw mechanism

First, we will consider a 331ISS model based on the original 331RHN model given in Ref. [24], where active neutrino masses and oscillations are generated from the ISS mechanism. The quark sector and  $SU(3)_C$  representations are irrelevant in this work, hence are omitted here. The electric charge operator corresponding to the gauge group  $SU(3)_L \times U(1)_X$  is  $Q = T_3 - \frac{1}{\sqrt{3}}T_8 + X$ , where  $T_{3,8}$  are diagonal  $SU(3)_L$  generators. Each lepton family consists

of a  $SU(3)_L$  triplet  $\psi_{aL} = (\nu_a, e_a, N_a)_L^T \sim (3, -\frac{1}{3})$ , and a right-handed charged lepton  $e_{aR} \sim (1, -1)$  with  $a = 1, 2, 3$ . Each left-handed neutrino  $N_{aL} = (N_{aR})^c$  implies a new right-handed neutrino beyond the SM. Three Higgs triplets are  $\rho = (\rho_1^+, \rho^0, \rho_2^+)^T \sim (3, \frac{2}{3})$ ,  $\eta = (\eta_1^0, \eta^-, \eta_2^0)^T \sim (3, -\frac{1}{3})$ , and  $\chi = (\chi_1^0, \chi^-, \chi_2^0)^T \sim (3, -\frac{1}{3})$ . The necessary VEVs for generating all tree level quark masses are:  $\langle \rho \rangle = (0, \frac{v_1}{\sqrt{2}}, 0)^T$ ,  $\langle \eta \rangle = (\frac{v_2}{\sqrt{2}}, 0, 0)^T$  and  $\langle \chi \rangle = (0, 0, \frac{w}{\sqrt{2}})^T$ . Gauge bosons in this model get masses through the covariant kinetic term of Higgs boson

$$\mathcal{L}^H = \sum_{H=\chi, \eta, \rho} (D_\mu H)^\dagger (D_\mu H),$$

where the covariant derivative for the electroweak symmetry is defined as

$$D_\mu = \partial_\mu - igW_\mu^a T^a - g_X T^9 X_\mu, \quad a = 1, 2, \dots, 8, \quad (1)$$

and  $T_9 \equiv \frac{I_3}{\sqrt{6}}$  and  $\frac{1}{\sqrt{6}}$  for (anti)triplets and singlets [27]. It can be identified that

$$g = e s_W, \quad \frac{g_X}{g} = \frac{3\sqrt{2}s_W}{\sqrt{3 - 4s_W^2}}, \quad (2)$$

where  $e$  and  $s_W$  are respective the electric charge and sine of the Weiberg angle,  $s_W^2 \simeq 0.231$ .

The model includes two pairs of singly charged gauge bosons, denoted as  $W^\pm$  and  $Y^\pm$ , defined as

$$\begin{aligned} W_\mu^\pm &= \frac{W_\mu^1 \mp iW_\mu^2}{\sqrt{2}}, \quad m_W^2 = \frac{g^2}{4} (v_1^2 + v_2^2), \\ Y_\mu^\pm &= \frac{W_\mu^6 \pm iW_\mu^7}{\sqrt{2}}, \quad m_Y^2 = \frac{g^2}{4} (w^2 + v_1^2). \end{aligned} \quad (3)$$

The bosons  $W^\pm$  are identified with the SM one, leading to  $v_1^2 + v_2^2 \equiv v^2 = (246\text{GeV})^2$ . We will consider indetail below the simple case  $v_1 = v_2 = v/\sqrt{2} = \sqrt{2}m_W/g$  given in [6, 26].

The two global symmetries, namely normal and new lepton numbers denoted as  $L$  and  $\mathcal{L}$  respectively were introduced. They relate with each other by [24, 25]:  $L = \frac{4}{\sqrt{3}}T_8 + \mathcal{L}$ . Detailed values of nonzero lepton numbers  $L$  and  $\mathcal{L}$  are listed in Table I.

Fields	$N_L$	$\nu_L$	$e_L$	$e_R$	$\rho_2^+$	$\eta_2^0$	$\chi_1^0$	$\chi^-$	Fields	$\chi$	$\eta$	$\rho$	$\psi_{aL}$	$e_{aR}$
$L$	-1	1	1	1	-2	-2	2	2	$\mathcal{L}$	$\frac{4}{3}$	$\frac{2}{3}$	$\frac{2}{3}$	$\frac{1}{3}$	1

TABLE I: Nonzero lepton number  $L$  (left) and  $\mathcal{L}$  (right) of leptons and Higgs bosons in the 331RHN

All tree level lepton mass terms come from the following Yukawa part

$$\mathcal{L}_l^Y = -h_{ab}^e \overline{\psi_{aL}} \rho e_{bR} + h_{ab}^\nu \epsilon^{ijk} \overline{(\psi_{aL})_i} (\psi_{bL})_j^c \rho_k^* + \text{H.c.} \quad (4)$$

where  $\epsilon^{ijk}$  is the antisymmetric tensor,  $\epsilon^{123} = 1$ ;  $(\psi_{aL})^c \equiv ((\nu_{aL})^c, (e_{aL})^c, (N_{aL})^c)^T$ ; and  $h^\nu$  is an antisymmetric matrix:  $h_{ab}^\nu = -h_{ba}^\nu$ . The first term of (4) generates charged lepton masses  $m_a$  satisfying  $h_{ab}^e \equiv \sqrt{2} \delta_{ab} m_a / v_1$ , in order to avoid large lepton flavor violating (LFV) processes at the tree level. The second term in (4) is expanded as follows:

$$h_{ab}^\nu \epsilon^{ijk} \overline{(\psi_{aL})_i} (\psi_{bL})_j^c \rho_k^* = 2h_{ab}^\nu \left[ -\overline{e_{aL}} (\nu_{bL})^c \rho_2^- - \overline{\nu_{aL}} (N_{bL})^c \rho^{0*} + \overline{e_{aL}} (\nu_{bL})^c \rho_1^- \right], \quad (5)$$

where we have used the equality  $\overline{N_{aL}} (\nu_{bL})^c = \overline{\nu_{bL}} (N_{aL})^c, \dots$ . The second term in the last line of (5) contributes a Dirac neutrino mass term  $-\mathcal{L}_{\text{mass}}^\nu = \overline{\nu_L} m_D N_R + \text{h.c.}$ , where  $\nu_L \equiv (\nu_{1L}, \nu_{2L}, \nu_{3L})^T$ ,  $N_R \equiv ((N_{1L})^c, (N_{2L})^c, (N_{3L})^c)^T$ , and  $(m_D)_{ab} \equiv \sqrt{2} v_1 h_{ab}^\nu$ . The model can predict mass spectrum consistent with current neutrino data [16] when loop corrections are included, where all new neutrinos are very light [24]. As a result, they will give suppressed LFV decay rates.

Now we consider an 331ISS model as an extension of the above 331RHN model, where three right-handed neutrinos which are gauge singlets,  $X_{aR} \sim (1, 0)$ ,  $a = 1, 2, 3$  are added. Now tree level neutrino masses and mixing angles arise from the ISS mechanism. Requiring that  $\mathcal{L}$  is only soft-broken, the additional Yukawa part is:

$$-\mathcal{L}_{X_R} = Y_{ab} \overline{\psi_{aL}} \chi X_{bR} + \frac{1}{2} (\mu_X)_{ab} \overline{(X_{aR})^c} X_{bR} + \text{h.c.}, \quad (6)$$

where  $\mu_X$  is a  $3 \times 3$  symmetric matrix and  $L(X_{aR}) = \mathcal{L}(X_{aR}) = -1$ . The last term in (6) is the only one violated both  $L$  and  $\mathcal{L}$ , hence can be assumed to be small, exactly the case appearing in the inverse seesaw models. The first term generates mass for heavy neutrinos, resulting in a very consistent consequence of large Yukawa coupling  $Y_{ab}$  with  $SU(3)_L$  Higgs triplets. In addition, the inverse seesaw mechanism allows large entries of Dirac mass matrix  $m_D$  originated from (4), which are completely opposite to the well-known requirement in the 331RHN.

In the basis  $\nu'_L = (\nu_L, N_L, (X_R)^c)^T$  and  $(\nu'_L)^c = ((\nu_L)^c, (N_L)^c, X_R)^T$ , (4) and (6) gives a neutrino mass term with the block form

$$-L_{\text{mass}}^\nu = \frac{1}{2} \overline{\nu'_L} M^\nu (\nu'_L)^c + \text{h.c.}, \text{ where } M^\nu = \begin{pmatrix} 0 & m_D & 0 \\ m_D^T & 0 & M_R \\ 0 & M_R^T & \mu_X \end{pmatrix}, \quad (7)$$

where  $M_R$  is a  $3 \times 3$  matrix having  $(M_R)_{ab} \equiv Y_{ab} \frac{w}{\sqrt{2}}$  with  $a, b = 1, 2, 3$ . Neutrino sub-bases are denoted as  $\nu_R = ((\nu_{1L})^c, (\nu_{2L})^c, (\nu_{3L})^c)^T$ ,  $N_R = ((N_{1L})^c, (N_{2L})^c, (N_{3L})^c)^T$ , and  $X_L = ((X_{1R})^c, (X_{2R})^c, (X_{3R})^c)^T$ .

The matrix  $M^\nu$  can be written in the normal seesaw form,

$$M^\nu = \begin{pmatrix} 0 & M_D \\ M_D^T & M_N \end{pmatrix}, \text{ where } M_D \equiv (m_D, 0), \text{ and } M_N = \begin{pmatrix} 0 & M_R \\ M_R^T & \mu_X \end{pmatrix}. \quad (8)$$

The mass matrix  $M^\nu$  is diagonalized by a  $9 \times 9$  unitary matrix  $U^\nu$  [18, 19],

$$U^{\nu T} M^\nu U^\nu = \hat{M}^\nu = \text{diag}(m_{n_1}, m_{n_2}, \dots, m_{n_9}) = \text{diag}(\hat{m}_\nu, \hat{M}_N), \quad (9)$$

where  $m_{n_i}$  ( $i = 1, 2, \dots, 9$ ) are mass eigenvalues of the 9 mass eigenstates  $n_{iL}$ , i.e. physical states of neutrinos; and  $\hat{m}_\nu = \text{diag}(m_{n_1}, m_{n_2}, m_{n_3})$  and  $\hat{M}_N = \text{diag}(m_{n_4}, m_{n_5}, \dots, m_{n_9})$ . They correspond to the masses of the three active neutrinos  $n_{aL}$  ( $a = 1, 2, 3$ ) and six extra neutrinos  $n_{iL}$  ( $i = 4, 5, \dots, 9$ ). The relation between the flavor and mass eigenstates are

$$\nu'_L = U^{\nu*} n_L, \quad \text{and } (\nu'_L)^c = U^\nu (n_L)^c, \quad (10)$$

where  $n_L \equiv (n_{1L}, n_{2L}, \dots, n_{9L})^T$  and  $(n_L)^c \equiv ((n_{1L})^c, (n_{2L})^c, \dots, (n_{9L})^c)^T$ .

A four-component (Dirac) spinor  $n_i$  are defined as  $n_i \equiv (n_{iL}, (n_{iL})^c)^T = n_i^c = (n_i)^c$ , where chiral components are  $n_{L,i} \equiv P_L n_i$  and  $n_{R,i} \equiv P_R n_i = (n_{L,i})^c$ , where  $P_{L,R} = \frac{1 \pm \gamma_5}{2}$  are chiral operators. The similar definitions for the original neutrino states are  $\nu_a \equiv (\nu_{L,a}, (\nu_{L,a})^c)^T$ ,  $\nu_a \equiv (N_{L,a}, (N_{L,a})^c)^T$ ,  $X_I \equiv ((X_{R,I})^c, X_{R,I})^T$ , and  $\nu' = (\nu, N)^T$ . The relations in (10) are

$$P_L \nu'_i = \nu'_{iL} = U_{ij}^{\nu*} n_{jL}, \text{ and } P_R \nu'_i = \nu'_{iR} = U_{ij}^\nu n_{jR}, \quad i, j = 1, 2, \dots, 9. \quad (11)$$

In general,  $U^\nu$  is written in the form [20],

$$U^\nu = \Omega \begin{pmatrix} U & \mathbf{O} \\ \mathbf{O} & V \end{pmatrix}, \quad (12)$$

where  $\mathbf{O}$  is a  $3 \times 6$  null matrix;  $U$ ,  $V$ , and  $\Omega$  are  $3 \times 3$ ,  $6 \times 6$  and  $9 \times 9$  unitary matrices, respectively. The  $\Omega$  can be formally written as

$$\Omega = \exp \begin{pmatrix} \mathbf{O} & R \\ -R^\dagger & \mathbf{O} \end{pmatrix} = \begin{pmatrix} 1 - \frac{1}{2} R R^\dagger & R \\ -R^\dagger & 1 - \frac{1}{2} R^\dagger R \end{pmatrix} + \mathcal{O}(R^3), \quad (13)$$

where  $R$  is a  $3 \times 6$  matrix with the maximal absolute value of all entries  $|R|$  satisfying  $|R| < 1$ . The matrix  $U = U_{\text{PMNS}}$  is the Pontecorvo-Maki-Nakagawa-Sakata (PMNS) matrix [21]:

$$U_{\text{PMNS}} = \begin{pmatrix} c_{12}c_{13} & s_{12}c_{13} & s_{13}e^{-i\delta} \\ -s_{12}c_{23} - c_{12}s_{23}s_{13}e^{i\delta} & c_{12}c_{23} - s_{12}s_{23}s_{13}e^{i\delta} & s_{23}c_{13} \\ s_{12}s_{23} - c_{12}c_{23}s_{13}e^{i\delta} & -c_{12}s_{23} - s_{12}c_{23}s_{13}e^{i\delta} & c_{23}c_{13} \end{pmatrix} \text{diag}(1, e^{i\frac{\alpha}{2}}, e^{i\frac{\beta}{2}}), \quad (14)$$

and  $c_{ab} \equiv \cos \theta_{ab}$ ,  $s_{ab} \equiv \sin \theta_{ab}$ . The Dirac phase  $\delta$  and Majorana phases  $\alpha, \beta$  will be fixed as  $\delta = \pi, \alpha = \beta = 0$ . In the normal hierarchy scheme, the best-fit values of neutrino oscillation parameters are given as [16]:

$$\begin{aligned} \Delta m_{21}^2 &= 7.370 \times 10^{-5} \text{ eV}^2, & \Delta m^2 &= 2.50 \times 10^{-3} \text{ eV}^2, \\ s_{12}^2 &= 0.297, & s_{23}^2 &= 0.437, & s_{13}^2 &= 0.0214, \end{aligned} \quad (15)$$

where  $\Delta m_{21}^2 = m_{n_2}^2 - m_{n_1}^2$  and  $\Delta m^2 = m_{n_3}^2 - \frac{\Delta m_{21}^2}{2}$ . Because  $v_1 \ll w$ , gives a reasonable condition  $|M_D| \ll |M_N|$ , where  $|M_D|$  and  $|M_N|$  denote characteristic scales of  $M_D$  and  $M_N$ . Hence the following seesaw relations are valid [20]

$$R^* \simeq (-m_D M^{-1}, \quad m_D (M_R^T)^{-1}), \quad (16)$$

$$m_D M^{-1} m_D^T \simeq m_\nu \equiv U_{\text{PMNS}}^* \hat{m}_\nu U_{\text{PMNS}}^\dagger, \quad (17)$$

$$V^* \hat{M}_N V^\dagger \simeq M_N + \frac{1}{2} R^T R^* M_N + \frac{1}{2} M_N R^\dagger R, \quad (18)$$

where

$$M \equiv M_R \mu_X^{-1} M_R^T. \quad (19)$$

In the model under consideration, the Dirac neutrino mass matrix  $m_D$  must be antisymmetric, equivalently,  $m_D$  has only three independent parameters  $x_{12}, x_{23}$  and  $z$ ,

$$m_D \equiv z \begin{pmatrix} 0 & x_{12} & x_{13} \\ -x_{12} & 0 & 1 \\ -x_{13} & -1 & 0 \end{pmatrix}, \quad (20)$$

where  $z = \sqrt{2} v_1 h_{23}^\nu$ . In contrast, the  $m_\nu$  in (17) is symmetric  $(m_\nu)_{ij} = (m_\nu)_{ji}$ . The equality (17) gives

$$0 = (m_\nu)_{ij} - (m_\nu)_{ji} \sim x_{12} [(M^{-1})_{12} - (M^{-1})_{21}] + x_{13} [(M^{-1})_{13} - (M^{-1})_{31}] + (M^{-1})_{23} - (M^{-1})_{32},$$

with  $i, j = 1, 2, 3$ . This means that a symmetric matrix  $M$  will give a right antisymmetric matrix  $m_D$ . To fit neutrino data, there must exist matrices  $M$  and  $m_D$  that satisfy the first equality in (17). Here we choose  $M$  to be symmetric for simplicity. There must exist some sets of  $z, x_{12}, x_{13}$  and  $M_{ij}$  ( $i \leq j \leq 3$ ) that satisfy six following equations  $(m_D M^{-1} m_D^T)_{ij} = (m_\nu)_{ij}$  with  $i \leq j \leq 3$ . From three Eqs. with  $i = j = 1, 2, 3$ , we can write  $(M^{-1})_{ii}$  as three functions of  $z, x_{12}, x_{13}$ , and  $(M^{-1})_{ij}$  ( $i \neq j$ ). Inserting them into the three remaining equalities, and taking some intermediate steps we obtain

$$\begin{aligned} -(m_\nu)_{13}x_{12} + (m_\nu)_{12}x_{13} &= (m_\nu)_{11}, \\ -(m_\nu)_{23}x_{12} + (m_\nu)_{22}x_{13} &= (m_\nu)_{12}, \\ -(m_\nu)_{33}x_{12} + (m_\nu)_{23}x_{13} &= (m_\nu)_{13}, \end{aligned} \quad (21)$$

where we exclude the case of  $x_{12}, x_{13} = 0$ . Solving above three equations leads to two solutions of  $x_{12,23}$  and a strict relation among  $(m_\nu)_{ij}$ :

$$\begin{aligned} x_{12} &= \frac{(m_\nu)_{11}(m_\nu)_{23} - (m_\nu)_{13}(m_\nu)_{12}}{(m_\nu)_{12}(m_\nu)_{33} - (m_\nu)_{13}(m_\nu)_{23}}, \\ x_{13} &= \frac{(m_\nu)_{11}(m_\nu)_{33} - (m_\nu)_{13}^2}{(m_\nu)_{12}(m_\nu)_{33} - (m_\nu)_{13}(m_\nu)_{23}}, \\ 0 &= (m_\nu)_{11}(m_\nu)_{23}^2 + (m_\nu)_{22}(m_\nu)_{13}^2 + (m_\nu)_{33}(m_\nu)_{12}^2 \\ &\quad - (m_\nu)_{11}(m_\nu)_{22}(m_\nu)_{33} - 2(m_\nu)_{12}(m_\nu)_{13}(m_\nu)_{23}. \end{aligned} \quad (22)$$

Interestingly, the last relation in (22) allow us predicting possible values of the unknown neutrino mass based on the identification given in (17). Using the experimental data (15), we derive that  $m_{\nu_1} = 0$  in the normal hierarchy scheme. The Dirac matrix now depends on only  $z$ :

$$m_D \simeq z \times \begin{pmatrix} 0 & 0.545 & 0.395 \\ -0.545 & 0 & 1 \\ -0.395 & -1 & 0 \end{pmatrix}. \quad (23)$$

The above discussion also gives  $M = \text{diag}(10^{10}z^2, 7.029 \times 10^{10}z^2, -2.377 \times 10^{11}z^2)$  for a diagonal  $M_R$ . In this work, we also consider a simple case where  $M_R$  is diagonal and all elements are positive. We also assume that  $|m_\nu| < \mu_X \ll |m_D| < |M_R|$ . We then derive that heavy neutrino masses are approximately equal to entries of  $M_R$ , as given in Eq. (19). But this approximation is not very good for investigating the LFVHD, where the



divergent cancellation in numerical computation is strictly forced. Instead, we will use the numerical solutions of heavy neutrino masses as well as the mixing matrix  $U^\nu$  so that total divergent part vanishes in the final numerical results. This treatment will avoid unphysical contributions originated from divergent parts.

There is another parameterization was shown in Ref. [9], that can be applied to the general cases of non-zero  $\delta$  as well as the both inverse and normal hierarchy cases of active neutrino masses. With the aim of finding regions with large LfVHD we will choose a simple case of  $m_D$  given in Eq. (23).

For simplicity in numerical study, we will consider the diagonal matrix  $M_R$  in the degenerate case  $M_R = M_{R_1} = M_{R_2} = M_{R_3} \equiv k \times z$ . The parameter  $k$  will be fixed for some small values resulting in large LfVHD effects. The total neutrino mass matrix in Eq. (7) depend on only the free parameter  $z$ . The heavy neutrino masses and the matrix  $U^\nu$  can be solved numerically, which is not affected by  $z$  because  $|\mu_X| \ll z$ .

Using the exact numerical solutions of neutrino masses and mixing matrix  $U^\nu$  for our investigation, we emphasize that the masses and mixing parameters of active neutrino masses derived from the numerical diagonalization the matrix  $M^\nu$  given in Eq. (7) should satisfy the  $3\sigma$  constraint of the experimental data. In contrast, neutrino masses and mixing parameters defining the matrix  $m_\nu$  in Eq. (17), which is used to calculate matrix  $m_D$ , are considered as free parameters. In other words, the experimental values of neutrino masses and mixing parameters are only used to estimate the ranges of free parameters determine the mass matrix  $M^\nu$ . After that, it is diagonalized numerically to find the neutrino masses as well as the mixing matrix  $U^\nu$ . The mixing parameters will be calculated from the the matrix  $U_{\text{PMNS}}$  relating with  $U^\nu$  by the relation (12). Requiring that the expansion of  $\Omega$  in Eq. (13) and the inverse seesaw condition  $|\mu_X| > m_{n_3}$  are valid, we find that small values of  $k > 1$  are allowed. In particular, we find that if three mixing parameters are fixed at the three respective center values, the two inputs of active neutrino masses maybe outside but very close to the  $3\sigma$  ranges with  $k = 5$ . When  $k \geq 5.5$ , we always find the input lying in the  $3\sigma$  ranges of experimental data that produce the consistent numerical solutions of active neutrino masses. When  $k \geq 9$ , the input corresponding to all center values given in (15) always produces the numerical solutions lying in the  $3\sigma$  ranges of experimental data.

The LfVHD rates depend strongly on the unitary of the mixing matrix  $U^\nu$  and heavy neutrino masses. On the other hand, they are affected weakly by the requirement that solu-

tions of active neutrino masses as well as mixing parameters satisfying the  $3\sigma$  experimental data. Hence we will use matrix  $m_D$  given in Eq. (23) and  $k \geq 5.5$  for numerical investigation. We checked numerically that our choice produces reasonable values of neutrino data close to the  $3\sigma$  ranges mentioned above.

## B. Higgs and gauge bosons

To study the Higgs LFV effects, we will choose the simple case of the Higgs potential discussed on [6, 26], namely

$$\begin{aligned} \mathcal{V} = & \mu_1^2 (\rho^\dagger \rho + \eta^\dagger \eta) + \mu_2^2 \chi^\dagger \chi + \lambda_1 (\rho^\dagger \rho + \eta^\dagger \eta)^2 + \lambda_2 (\chi^\dagger \chi)^2 + \lambda_{12} (\rho^\dagger \rho + \eta^\dagger \eta) (\chi^\dagger \chi) \\ & - \sqrt{2} f (\varepsilon_{ijk} \eta^i \rho^j \chi^k + \text{h.c.}), \end{aligned} \quad (24)$$

where  $f$  is a mass parameter and is assumed to be real. The detailed calculation for finding masses and mass eigenstates of Higgs bosons are presented in [6, 26], where the minimum condition results in  $v_1 = v_2$ . We will list here only part involving directly with LFVHD.

The model contains two pairs of singly charged Higgs boson  $H_{1,2}^\pm$  and goldstone bosons of the gauge bosons  $W^\pm$  and  $Y^\pm$ , which are denoted as  $G_W^\pm$  and  $G_Y^\pm$ , respectively. The masses of all charged Higgs bosons are  $m_{H_1^\pm}^2 = fw(t_\theta^2 + 1)$ ,  $m_{H_2^\pm}^2 = 2fw$ , and  $m_{G_W^\pm}^2 = m_{G_Y^\pm}^2 = 0$ , where  $t_\theta = v_2/w$ . Relations between original charged Higgs components are:

$$\begin{pmatrix} \rho_1^\pm \\ \eta^\pm \end{pmatrix} = \frac{1}{\sqrt{2}} \begin{pmatrix} -1 & 1 \\ 1 & 1 \end{pmatrix} \begin{pmatrix} G_W^\pm \\ H_2^\pm \end{pmatrix}, \quad \begin{pmatrix} \rho_2^\pm \\ \chi^\pm \end{pmatrix} = \begin{pmatrix} -s_\theta & c_\theta \\ c_\theta & s_\theta \end{pmatrix} \begin{pmatrix} G_Y^\pm \\ H_1^\pm \end{pmatrix}. \quad (25)$$

The neutral scalars are expanded as

$$\begin{aligned} \rho^0 &= \frac{1}{\sqrt{2}}(v_1 + S_1 + iA_1), \quad \eta_1^0 = \frac{1}{\sqrt{2}}(v_2 + S_2 + iA_2), \quad \chi_2^0 = \frac{1}{\sqrt{2}}(w + S'_3 + iA'_3), \\ \eta_2^0 &= \frac{1}{\sqrt{2}}(S'_2 + iA'_2), \quad \chi_1^0 = \frac{1}{\sqrt{2}}(S_3 + iA_3). \end{aligned} \quad (26)$$

There are four physical CP-even Higgs bosons  $h_{1,2,3,4}^0$  and a goldstone boson of the non-hermitian gauge boson. The neutral Higgs components relevant with this work are defined via

$$\begin{pmatrix} S_1 \\ S_2 \\ S'_3 \end{pmatrix} = \begin{pmatrix} -\frac{c_\alpha}{\sqrt{2}} & \frac{s_\alpha}{\sqrt{2}} & \frac{1}{\sqrt{2}} \\ -\frac{c_\alpha}{\sqrt{2}} & \frac{s_\alpha}{\sqrt{2}} & -\frac{1}{\sqrt{2}} \\ s_\alpha & c_\alpha & 0 \end{pmatrix} \begin{pmatrix} h_1^0 \\ h_2^0 \\ h_3^0 \end{pmatrix}, \quad (27)$$

where  $s_\alpha = \sin \alpha$  and  $c_\alpha = \cos \alpha$  and they are defined by

$$s_\alpha = \frac{(4\lambda_1 - m_{h_1^0}^2/v_2^2)t_\theta}{r}, \quad c_\alpha = \frac{\sqrt{2}(\lambda_{12} - \frac{f}{w})}{r},$$

$$r = \sqrt{2\left(\lambda_{12} - \frac{f}{w}\right)^2 + \left(4\lambda_1 - m_{h_1^0}^2/v_2^2\right)^2 t_\theta^2}. \quad (28)$$

There is one neutral CP-even Higgs boson  $h_1^0$  with mass having electroweak scale,

$$m_{h_1^0}^2 = \frac{w^2}{2} \left[ 4\lambda_1 t_\theta^2 + 2\lambda_2 + \frac{ft_\theta^2}{w} - \sqrt{\left(2\lambda_2 + \frac{ft_\theta^2}{w} - 4\lambda_1 t_\theta^2\right)^2 + 8t_\theta^2 \left(\frac{f}{w} - \lambda_{12}\right)^2} \right]. \quad (29)$$

The decoupling limit  $t_\theta \ll 1$  ( $v_1 \ll w$ ) gives  $m_{h_1^0}^2 \sim \mathcal{O}(m_W^2)$  and  $s_\alpha \simeq 0$  [26], resulting the couplings similarly to those predicted by the SM, see Table II. Hence  $h_1^0$  is identified with the SM-like Higgs boson found at LHC.

### III. COUPLINGS AND ANALYTIC FORMULAS INVOLVED WITH LFVHD

#### A. Couplings

This section Yukawa couplings will be presented in terms of  $U^\nu$  and physical neutrino masses. From this, amplitudes and the LFVHD rate are formulated in terms of physical masses and mixing parameters. The equality derived from (9),  $M^\nu = U^{\nu*} \hat{M}^\nu U^{\nu\dagger}$ , gives

$$M_{ab}^\nu = \left( U^{\nu*} \hat{M}^\nu U^{\nu\dagger} \right)_{ab} = 0 \rightarrow U_{ak}^{\nu*} U_{bk}^{\nu*} m_{n_k} = 0,$$

$$\sqrt{2} v_1 h_{ab}^\nu = (m_D)_{ab} = (M^\nu)_{a(b+3)} = (U^{\nu*} \hat{M}^\nu U^{\nu\dagger})_{a(b+3)} = U_{ak}^{\nu*} U_{(b+3)k}^{\nu*} m_{n_k},$$

$$\frac{w}{\sqrt{2}} Y_{ab} = (M_R)_{ab} = (M^\nu)_{(a+3)(b+6)} = U_{(a+3)k}^{\nu*} U_{(b+6)k}^{\nu*} m_{n_k}, \quad (30)$$

where  $a, b = 1, 2, 3$ , and sum is taken over  $k = 1, 2, \dots, 9$ .

Relevant couplings in the first term of Lagrangian (4) are

$$- h_{ab}^e \overline{\psi_{aL} \rho e_{bR}} + \text{h.c.} = - \frac{g m_a}{m_W} [\overline{\nu_{aL}} e_{aR} \rho_1^+ + \overline{e_{aL}} e_{aR} \rho^0 + \overline{N_{aL}} e_{aR} \rho_2^+ + \text{h.c.}]$$

$$\supset \frac{g m_a c_\alpha}{2 m_W} h_1^0 \overline{e_a} e_a - \frac{g m_a}{m_W} [c_\theta (U_{(a+3)i}^\nu \overline{n_i} P_R e_a H_1^+ + U_{(a+3)i}^{\nu*} \overline{e_a} P_L n_i H_1^-)]$$

$$- \frac{g m_a}{\sqrt{2} m_W} [(U_{ai}^\nu \overline{n_i} P_R e_a H_2^+ + U_{ai}^{\nu*} \overline{e_a} P_L n_i H_2^-)]. \quad (31)$$

Relevant couplings in the second term of Lagrangian (4) are

$$h_{ab}^\nu \epsilon^{ijk} \overline{(\psi_{aL})_i} (\psi_{bL})_j^c \rho_k^* + \text{h.c.}$$

$$\begin{aligned}
&= 2h_{ab}^\nu \left[ -\overline{e_{aL}}(\nu_{bL})^c \rho_2^- - \overline{\nu_{aL}}(N_{bL})^c \rho^{0*} + \overline{e_{aL}}(\nu_{bL})^c \rho_1^- \right] \\
&= \frac{gc_\alpha}{2m_W} h_1^0 \left[ \sum_{c=1}^3 U_{ci}^\nu U_{cj}^{\nu*} \overline{n_i} (m_{n_i} P_L + m_{n_j} P_R) n_j \right] \\
&- \frac{gc_\theta}{m_W} \left[ (m_D)_{ab} U_{bi}^\nu H_1^- \overline{e_a} P_R n_i + \text{h.c.} \right] + \frac{g}{\sqrt{2}m_W} \left[ (m_D)_{ab} U_{(b+3)i}^\nu H_2^- \overline{e_a} P_R n_i + \text{h.c.} \right], \quad (32)
\end{aligned}$$

where the last line is derived following calculation in Ref. [19]:  $\overline{\nu_L} M_D ((N_L)^c, X_R)^T \leftrightarrow \overline{\nu_{aL}} (M_D)_{aI} N_{IR}$ . The first term in (6) gives the following couplings:

$$\begin{aligned}
&- Y_{ab} \overline{\psi_{aL}} \chi X_{bR} + \text{h.c.} \\
&= -\frac{\sqrt{2}}{w} (M_R)_{ab} \left[ \overline{\nu_{aL}} \chi_1^0 + \overline{e_{aL}} \chi^- + \overline{N_{aL}} \chi_2^0 \right] X_{bR} + \text{h.c.} \\
&\supset -\frac{gt_\theta}{\sqrt{2}m_W} (M_R)_{ab} \left[ s_\alpha U_{(a+3)i}^\nu U_{(b+6)j}^\nu \overline{n_i} P_R n_j h_1^0 + \sqrt{2} s_\theta U_{(b+6)i}^\nu \overline{e_a} P_R n_i H_1^- + \text{h.c.} \right], \quad (33)
\end{aligned}$$

where we have used  $t_\theta = v_1/w \rightarrow 1/w = t_\theta/v_1 = gt_\theta/(\sqrt{2}m_W)$ . LFVHD couplings between leptons and charged gauge bosons ( $W^\pm, Y^\pm$ ) are

$$\begin{aligned}
\mathcal{L}^{\ell\ell V} &= \overline{\psi_{aL}} \gamma^\mu D_\mu \psi_{aL} \supset \frac{g}{\sqrt{2}} (\overline{e_{aL}} \gamma^\mu \nu_{aL} W_\mu^- + \overline{e_{aL}} \gamma^\mu N_{aL} Y_\mu^-) + \text{h.c.} \\
&= \frac{g}{\sqrt{2}} \left[ U_{ai}^{\nu*} \overline{e_a} \gamma^\mu P_L n_i W_\mu^- + U_{ai}^\nu \overline{n_i} \gamma^\mu P_L e_a W_\mu^+ \right. \\
&\quad \left. + U_{(a+3)i}^{\nu*} \overline{e_a} \gamma^\mu P_L n_i Y_\mu^- + U_{(a+3)i}^\nu \overline{n_i} \gamma^\mu P_L e_a Y_\mu^+ \right], \quad (34)
\end{aligned}$$

where  $D_\mu = \partial_\mu - \frac{ig}{2} (W_\mu^a \lambda^a + t \times (-\frac{1}{3}) B_\mu)$ ,  $\lambda_a$  ( $a = 1, 2, \dots, 8$ ) is a Gell-mann matrix, and  $t = g_X/g$ . Charged gauge bosons are  $W_\mu^\pm = \frac{W_\mu^1 \mp i W_\mu^2}{\sqrt{2}}$  and  $Y_\mu^\pm = \frac{W_\mu^6 \pm i W_\mu^7}{\sqrt{2}}$ .

By defining a symmetric coefficient  $\lambda_{ij}^0 = \lambda_{ji}^0$ , namely

$$\lambda_{ij}^0 = \sum_{c=1}^3 (U_{ci}^\nu U_{cj}^{\nu*} m_{n_i} + U_{ci}^{\nu*} U_{cj}^\nu m_{n_j}) - \sum_{c,d=1}^3 \sqrt{2} t_\alpha t_\theta (M_R^*)_{cd} [U_{(c+3)i}^{\nu*} U_{(d+6)j}^\nu + U_{(c+3)j}^{\nu*} U_{(d+6)i}^\nu],$$

the coupling  $h_1^0 \overline{n_i} n_j$  derived from (32) and (33) is written in the symmetric form  $\frac{gc_\alpha}{4m_W} h_1^0 \overline{n_i} [\lambda_{ij}^0 P_L + \lambda_{ij}^{0*} P_R] n_j$ , which gives a right vertex coupling based on the Feynman rules given in [22]. The Yukawa couplings of charged Higgs bosons are defined by

$$\begin{aligned}
\lambda_{ai}^{R,1} &= m_a U_{(a+3)i}^\nu, \quad \lambda_{ai}^{L,1} = \sum_{c=1}^3 [(m_D^*)_{ac} U_{ci}^{\nu*} + t_\theta^2 (M_R^*)_{ac} U_{(c+6)i}^{\nu*}], \\
\lambda_{ai}^{R,2} &= m_a U_{ai}^\nu, \quad \lambda_{ai}^{L,2} = -\sum_{c=1}^3 (m_D^*)_{ac} U_{(c+3)i}^{\nu*}, \quad (35)
\end{aligned}$$

Finally, all of the coupling involving with LFV processes are listed in the table II. The model predicts the following couplings are zero:  $h_1^0 W^\pm Y^\mp$ ,  $h_1^0 W^\pm H_{1,2}^\mp$ ,  $h_1^0 Y^\pm H_2^\mp$  and  $h_1^0 H_1^\pm H_2^\mp$ .

Vertex	Coupling
$h_1^0 \bar{e}_a e_a$	$\frac{igm_a}{2m_W} c_\alpha$
$h_1^0 \bar{n}_i n_j$	$\frac{igc_\alpha}{2m_W} \left( \lambda_{ij}^0 P_L + \lambda_{ij}^{0*} P_R \right)$
$H_1^+ \bar{n}_i e_b, H_1^- \bar{e}_a n_i$	$-\frac{igc_\theta}{m_W} \left( \lambda_{bi}^{L,1} P_L + \lambda_{bi}^{R,1} P_R \right), -\frac{igc_\theta}{m_W} \left( \lambda_{ai}^{L,1*} P_R + \lambda_{ai}^{R,1*} P_L \right)$
$H_2^+ \bar{n}_i e_b, H_2^- \bar{e}_a n_i$	$-\frac{ig}{\sqrt{2}m_W} \left( \lambda_{bi}^{L,2} P_L + \lambda_{bi}^{R,2} P_R \right), -\frac{ig}{\sqrt{2}m_W} \left( \lambda_{ai}^{L,2*} P_R + \lambda_{ai}^{R,2*} P_L \right)$
$W_\mu^+ \bar{n}_i e_b, W_\mu^- \bar{e}_a n_i$	$\frac{ig}{\sqrt{2}} U_{bi}^\nu \gamma^\mu P_L, \frac{ig}{\sqrt{2}} U_{ai}^{\nu*} \gamma^\mu P_L$
$Y_\mu^+ \bar{n}_i e_b, Y_\mu^- \bar{e}_a n_i$	$\frac{ig}{\sqrt{2}} U_{(b+3)i}^\nu \gamma^\mu P_L, \frac{ig}{\sqrt{2}} U_{(a+3)i}^{\nu*} \gamma^\mu P_L$
$H_1^+ h_1^0 Y_\mu^-, Y_\mu^+ H_1^- h_1^0$	$\frac{ig}{2\sqrt{2}} (c_\alpha c_\theta + \sqrt{2} s_\alpha s_\theta) (p_{h_1^0} - p_{H_1^+})^\mu, \frac{ig}{2\sqrt{2}} (c_\alpha c_\theta + \sqrt{2} s_\alpha s_\theta) (p_{H_1^-} - p_{h_1^0})^\mu$
$h_1^0 W_\mu^+ W_\nu^-$	$-igm_W c_\alpha g^{\mu\nu}$
$h_1^0 Y_\mu^+ Y_\nu^-$	$\frac{igm_Y}{\sqrt{2}} (\sqrt{2} s_\alpha c_\theta - c_\alpha s_\theta) g^{\mu\nu}$
$h_1^0 H_1^+ H_1^-$	$i\lambda_{H_1}^\pm = -iw \left[ s_\alpha c_\theta^2 \lambda_{12} + 2s_\alpha s_\theta^2 \lambda_2 - \sqrt{2} (2c_\alpha c_\theta^2 \lambda_1 + c_\alpha s_\theta^2 \lambda_{12}) t_\theta - \frac{\sqrt{2}}{v_3} f c_\alpha c_\theta s_\theta \right]$
$h_1^0 H_2^+ H_2^-$	$i\lambda_{H_2}^\pm = -iv_1 \left( -2\sqrt{2} c_\alpha \lambda_1 + \frac{s_\alpha v_3 \lambda_{12} + s_\alpha f}{v_1} \right)$

TABLE II: Couplings relating with the SM-like Higgs decay  $h_1^0 \rightarrow e_a e_b$  decays in the 331ISS model. All momenta in the Feynman rules corresponding to these vertices are incoming.

## B. Analytic formulas

The effective Lagrangian of the LFBVD of the SM-like Higgs boson  $h_1^0 \rightarrow e_a^\pm e_b^\mp$  is

$$\mathcal{L}^{\text{LFBVD}} = h_1^0 \left( \Delta_{(ab)L} \bar{e}_a P_L e_b + \Delta_{(ab)R} \bar{e}_a P_R e_b \right) + \text{H.c.},$$

where scalar factors  $\Delta_{(ab)L,R}$  arise from the loop contributions. In the unitary gauge, the one-loop Feynman diagrams contributing to this LFBVD amplitude are shown in Fig. 1.

The partial width of the decay is

$$\Gamma(h_1^0 \rightarrow e_a e_b) \equiv \Gamma(h_1^0 \rightarrow e_a^- e_b^+) + \Gamma(h_1^0 \rightarrow e_a^+ e_b^-) = \frac{m_{h_1^0}}{8\pi} (|\Delta_{(ab)L}|^2 + |\Delta_{(ab)R}|^2), \quad (36)$$

with the condition  $m_{h_1^0} \gg m_{a,b}$  and  $m_{a,b}$  being masses of muon and tau, respectively. The on-shell conditions for external particles are  $p_{1,2}^2 = m_{a,b}^2$  and  $p_{h_1^0}^2 \equiv (p_1 + p_2)^2 = m_{h_1^0}^2$ . The corresponding branching ratio is  $\text{Br}(h_1^0 \rightarrow e_a e_b) = \Gamma(h_1^0 \rightarrow e_a e_b) / \Gamma_{h_1^0}^{\text{total}}$  where  $\Gamma_{h_1^0}^{\text{total}} \simeq 4.1 \times 10^{-3} \text{ GeV}$  [16, 30]. The  $\Delta_{(ab)L,R}$  can be written as

$$\Delta_{(ab)L,R} = \sum_{i=1,5,7,8} \Delta_{(ab)L,R}^{(i)W} + \sum_{i=1}^{10} \Delta_{(ab)L,R}^{(i)Y}, \quad (37)$$

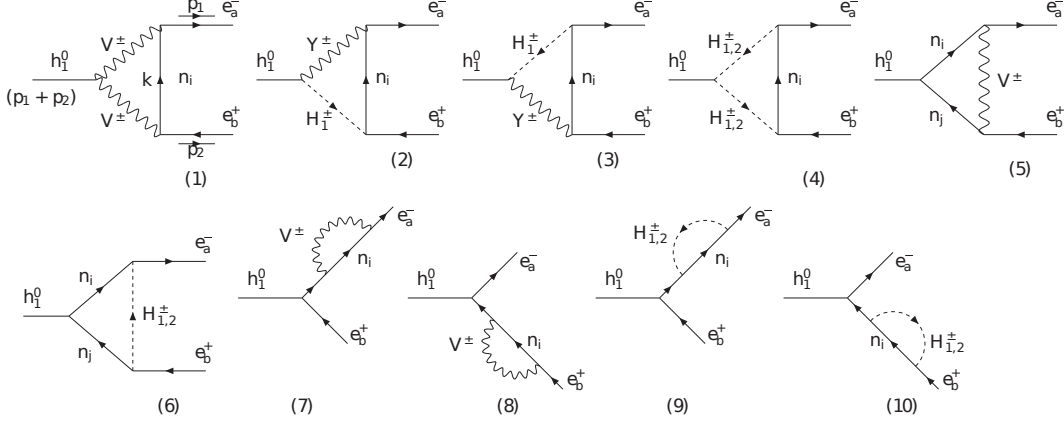


FIG. 1: One-loop Feynman diagrams contributing to the decay  $h_1^0 \rightarrow e_a e_b$  in the unitary gauge. Here  $V^\pm = W^\pm, Y^\pm$ .

where analytic forms of  $\Delta_{(ab)L,R}^{(i)W}$  and  $\Delta_{(ab)L,R}^{(i)Y}$  are shown in Appendix A. They can be calculated using the unitary gauge with the same techniques given in Refs. [6, 19]. We have crosschecked with form [23].

The divergence cancellation of in the total amplitude (37) is proved analytically in Appendix A, based on the following strict equality:

$$\begin{aligned}
 U^\nu (\hat{M}^\nu)^2 U^{\nu\dagger} &= (U^{\nu*} \hat{M}^\nu U^{\nu\dagger})^* U^{\nu*} \hat{M}^\nu U^{\nu\dagger} = M^{\nu*} M^\nu \\
 &= \begin{pmatrix} m_D^* m_D^T & 0 & m_D^* M_R \\ 0 & m_D^\dagger m_D + M_R^* M_R^T & M_R^* \mu_X \\ M_R^\dagger m_D^T & \mu_X^* M_R^T & M_R^\dagger M_R + \mu_X^* \mu_X \end{pmatrix} \quad (38)
 \end{aligned}$$

Because our formulas of  $\Delta_{(ab)L,R}^{(i)W}$  and  $\Delta_{(ab)L,R}^{(i)Y}$  are expressed as functions of physical masses and elements of mixing matrix  $U^\nu$ , the many elements in left hand side of the first line of Eq. (38) relate to the private divergent parts of  $\Delta_{(ab)L,R}^{(i)W}$  and  $\Delta_{(ab)L,R}^{(i)Y}$ , where those from charged Higgs and heavy gauged bosons relate to both  $(M^{\nu*} M^\nu)_{(a+3)(b+3)}$  and  $(M^{\nu*} M^\nu)_{(a+6)(b+6)}$  with  $a, b \leq 3$ . The cancellation in the total divergent part require that the physical heavy neutrino masses and  $U^\nu$  should be close to the exact values. For example, the heavy neutrino masses must be kept to the order of  $|O(R^2)|M_N$ , implying that the mixing matrix  $V$  in Eq. (18) is an exact solution. This condition is unlike the usual minimal version extended directly from the SM, because the LFVHD amplitude involves only the elements  $(M^{\nu*} M^\nu)_{ab}$ .

Many contributions listed in Eq. (37) are suppressed, hence can be ignored in numerical computation. From now on, we just focus on the decay  $h_1^0 \rightarrow \mu\tau$ , hence use the simplified

notation  $\Delta_{L,R} \equiv \Delta_{(23)L,R}$ . The decay  $h_1^0 \rightarrow e\tau$  has the similar properties so we do not need to discuss more explicitly. We can see that  $|\frac{\Delta_L}{\Delta_R}| \simeq \mathcal{O}\left(\frac{m_\mu}{m_\tau}\right)$ . In addition, We proved in the Appendix A that the following combinations are finite them selves:  $\Delta_{L,R}^{(1+5)W}$ ,  $\Delta_{L,R}^{(7+8)W}$ ,  $\Delta_{L,R}^{(4)YH_2}$ ,  $\Delta_{L,R}^{(6+9+10)YH_2}$ ,  $\Delta_{L,R}^{(4)YH_1}$ ,  $\Delta_{L,R}^{(7+8)Y}$ , and  $(\Delta_{L,R}^{(1+2+3+5)Y} + \Delta_{L,R}^{(6+9+10)YH_1})$ . With  $m_{\mu,\tau} \ll m_W$ , we have  $B_1^{(1)} + B_1^{(2)}$ ,  $B_1^{(2)} - B_0^{(2)} \simeq 0$ , hence  $\Delta_{L,R}^{(7+8)W}$ ,  $\Delta_{L,R}^{(7+8)Y} \simeq 0$ . The two contributions  $\Delta_{L,R}^{(4)YH_{1,2}^\pm}$  are also suppressed with large  $m_{H_2^\pm}$  for about few TeV.

The four diagrams (4), (6), (9) and (10) include contributions from both charged Higgs bosons. They are not affected significantly of the  $SU(3)_L$  scale  $m_Y$ , resulting in that they may enhance the partial decay widths of the LFVHD with small charged Higgs masses.

The regions of parameter space predicting large Brs of LFVHD are affected strongly by the current experimental data of  $\text{Br}(\mu \rightarrow e\gamma) < 4.2 \times 10^{-13}$  [8]. A very good approximate formula of this decay rate in the limit  $m_\mu, m_e \rightarrow 0$  is [12]

$$\text{Br}(\mu \rightarrow e\gamma) = \frac{12\pi^2}{G_F^2} |D_R|^2, \quad (39)$$

where  $G_F = g^2/(4\sqrt{2}m_W^2)$  and  $D_R$  is the one-loop contribution from charged gauge and Higgs boson mediations,  $D_R = D_R^W + D_R^Y + D_R^{H_1^\pm} + D_R^{H_2^\pm}$ . Analytics forms are

$$\begin{aligned} D_R^W &= -\frac{eg^2}{32\pi^2 m_W^2} \sum_{i=1}^9 U_{ai}^{\nu*} U_{bi}^\nu F(t_{iW}), \\ D_R^Y &= -\frac{eg^2}{32\pi^2 m_Y^2} \sum_{i=1}^9 U_{(a+3)i}^{\nu*} U_{(b+3)i}^\nu F(t_{iY}), \\ D_R^{H_k^\pm} &= -\frac{eg^2 f_k}{16\pi^2 m_W^2} \sum_{i=1}^9 \left[ \frac{\lambda_{ai}^{L,k*} \lambda_{bi}^{L,k}}{m_{H_k^\pm}^2} \times \frac{1 - 6t_{ik} + 3t_{ik}^2 + 2t_{ik}^3 - 6t_{ik}^2 \ln(t_{ik})}{12(t_{ik} - 1)^4} \right. \\ &\quad \left. + \frac{m_{n_i} \lambda_{ai}^{L,k*} \lambda_{bi}^{'R,k}}{m_{H_k^\pm}^2} \times \frac{-1 + t_{ik}^2 - 2t_{ik} \ln(t_{ik})}{2(t_{ik} - 1)^3} \right], \end{aligned} \quad (40)$$

where

$$\begin{aligned} b &= 2, \quad a = 1, \quad t_{iW} \equiv \frac{m_{n_i}^2}{m_W^2}, \quad t_{iY} \equiv \frac{m_{n_i}^2}{m_Y^2}, \quad t_{ik} \equiv \frac{m_{n_i}^2}{m_{H_k^\pm}^2}, \\ f_1 &\equiv \frac{1}{2}, \quad f_2 \equiv c_\theta^2, \quad \lambda_{bi}^{'R,1} \equiv U_{(b+3)i}^\nu, \quad \lambda_{bi}^{'R,2} \equiv U_{bi}^\nu, \\ F(x) &\equiv -\frac{10 - 43x + 78x^2 - 49x^3 + 4x^4 + 18x^3 \ln(x)}{12(x - 1)^4}. \end{aligned} \quad (41)$$

Because all charged Higgs bosons couple with heavy neutrinos through the Yukawa matrix  $h_{ab}^\nu$ , hence this matrix is strongly affected by the upper bound  $\mathcal{O}(10^{-13})$  of  $\text{Br}(\mu \rightarrow e\gamma)$ .

In fact, our numerical investigation shows that the allowed region with light charged Higgs masses are very narrow. A previous investigation of the  $\text{Br}(\mu \rightarrow e\gamma)$  in Ref. [9] showed that it is large from the prediction of the 331ISS, where the allowed regions discussed there were chosen safely that  $k \sim \mathcal{O}(10^3)$  and  $M_R \leq 1$  TeV, implying that  $z \sim \mathcal{O}(1)$  eV. Our formulas were checked to be consistent with these results. In general, the allowed regions is very strict, which satisfy one of the following conditions. First, the regions have small  $z$  while large  $|M_R|$  and  $m_{H_2^\pm}$ , implying  $k \gg 1$ , including those mainly discussed in Ref. [9]. Second, the regions allow large  $m_D$  and small  $k$ , but the strong destructive correlation between the two loop contributions of charged gauge and Higgs bosons must happen. These region were also concerned but not paid enough attention in Ref. [9]. They are very interesting because they predict large Brs of LFVHD and light particles such as new neutrinos and charged Higgs boson which could be found at LHC and planned colliders. Hence, our numerical investigation will focus on this case.

## IV. NUMERICAL DISCUSSION ON LFVHD

### A. Setup parameters

To investigate numerically the LFVHD of the SM-like Higgs boson, we will use the well-known experimental parameters [16]: the mass of  $W$  boson  $m_W = 80.385$  GeV; charged lepton masses:  $m_e = 5 \times 10^{-4}$  GeV,  $m_\mu = 0.105$  GeV,  $m_\tau = 1.776$  GeV; SM-like Higgs mass  $m_{h_1^0} = 125.1$  GeV; and the gauge coupling of the  $SU(2)_L$  symmetry  $g \simeq 0.651$ .

Combining with the discussion in Sec. II, the independent parameters are: the heavy neutrino mass scale  $M_R = \text{diag}(M_R, M_R, M_R)$ , the heavy gauge boson mass  $m_Y$  considered as  $SU(3)_L$  breaking scale, one charged Higgs boson mass  $m_{H_2^\pm}$ , the characteristic scale of  $m_D$  defined as the parameter  $z$ , and the two Higgs self couplings  $\lambda_{1,12}$ .

Other parameters can be calculated in terms of the above free ones, namely,

$$v_1 = v_2 = \frac{\sqrt{2}m_W}{g}, \quad s_\theta = \frac{m_W}{m_Y\sqrt{2}}, \quad w = \frac{2m_Y}{g c_\theta}, \quad f = \frac{g c_\theta m_{H_2^\pm}^2}{4m_Y}, \quad m_{H_1^\pm}^2 = \frac{m_{H_2^\pm}^2}{2}(t_\theta^2 + 1). \quad (42)$$

Apart from that, the mixing parameter  $\alpha$  of the neutral CP-even Higgs was defined in Eq.



(28). The Higgs-self-coupling  $\lambda_2$  is determined as [6]

$$\lambda_2 = \frac{t_\theta^2}{2} \left( \frac{m_{h_1^0}^2}{v_1} - \frac{m_{H_2^\pm}^2}{2w^2} \right) + \frac{\left( \lambda_{12} - \frac{m_{H_2^\pm}^2}{2w^2} \right)^2}{4\lambda_1 - \frac{m_{h_1^0}^2}{v_1^2}}. \quad (43)$$

In the model under consideration with the quark sector given in Refs. [24, 28], only the charged Higgs bosons  $H_2^\pm$  couple with all SM leptons and quarks. They have been searched at LHC in the direct production  $pp \rightarrow t(b)H^\pm$  then decay into two final fermion states [29]. But the specific constrains for them under the framework of the 3-3-1 models have not been mentioned yet, to the best of our knowledge. In stead, the lower bounds of their masses have been discussed recently based on recent data of neutral meson mixing  $B_0 - \bar{B}_0$ , where a reasonable lower bound of  $m_{H_2^\pm} \geq 480$  GeV was concerned [28].

The values of  $\lambda_{1,2,12}$  must satisfy theoretical conditions of unitarity and the Higgs potential must be bounded from below, as mentioned in [6]. The heavy charged gauge boson mass  $m_Y$  relating with recent lower constraint of neutral gauge boson  $Z'$  in this model.

For above reason, the default values of free parameters chosen for numerical investigation are as follows. Without loss of generality, the Higgs self couplings are fixed as  $\lambda_1 = 1$ ,  $\lambda_{12} = -1$ , which also guarantee that all couplings of the SM-like Higgs boson approach the SM limit when  $t_\theta \rightarrow 0$ . The default value  $m_Y = 4.5$  TeV satisfies all recent constraints [28, 31]. The parameter  $z$  will be considered in the range of perturbative limit  $z < 2\sqrt{\pi} \times v_1 \simeq 617$  GeV, in particularly we will fixed  $z = 50, 200, 400, 500$  and  $600$  [GeV]. Finally, charged Higgs mass  $m_{H_2^\pm}$  will be investigated mainly in the range from 300 GeV to  $5 \times 10^4$  GeV, where large values of LFVHD may appear.

## B. Numerical results

First, we reproduce the regions mentioned in Ref. [9], where  $M_R$  was chosen to be from hundreds GeV to 1 TeV and the scale of  $m_D$ , namely  $z$ , was few GeV, corresponding to  $k \gg 1$ . As a result, the respective regions of parameter space always satisfy the experimental bound of  $\text{Br}(\mu \rightarrow e\gamma)$  with large enough  $m_{H_2^\pm}$ . These regions are shown in Fig. 2 with fixed  $z = 1, 5, 10, 100$  and  $500$  GeV. All allowed regions, i.e. those satisfy the upper bound  $\text{Br}(\mu \rightarrow e\gamma) < 4.2 \times 10^{-13}$ , give small  $\text{Br}(h_1^0 \rightarrow \mu\tau) < \mathcal{O}(10^{-9})$ . In general, for larger  $k$  we

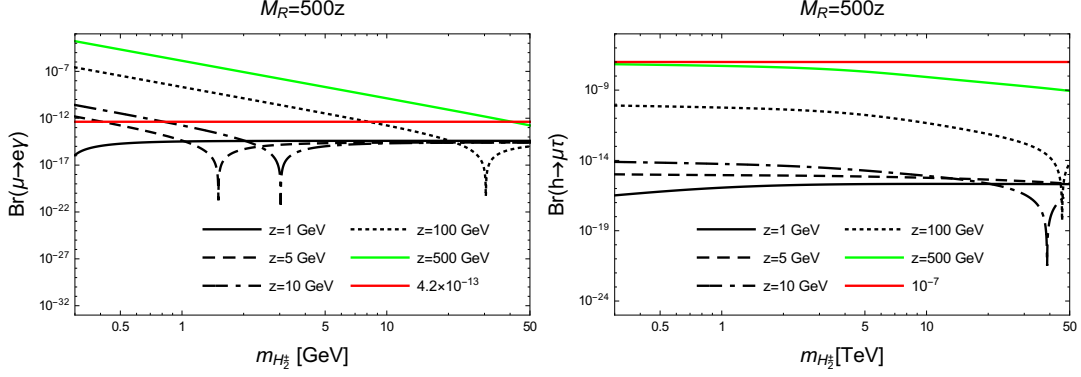


FIG. 2:  $\text{Br}(\mu \rightarrow e\gamma)$  (left) and  $\text{Br}(h_1^0 \rightarrow \mu\tau)$  (right) as functions of  $m_{H_2^\pm}$  with  $k = 500$ .

checked numerically that values of LFVHD Br will decrease significantly, hence we will not discuss any more.

With small values of  $k = 5.5$  and  $9$ , the dependence of both  $\text{Br}(\mu \rightarrow e\gamma)$  and  $\text{Br}(h \rightarrow \mu\tau)$  on  $m_{H_2^\pm}$  with fixed  $z$  are shown in Fig. 3. Most of the regions of the parameter space are

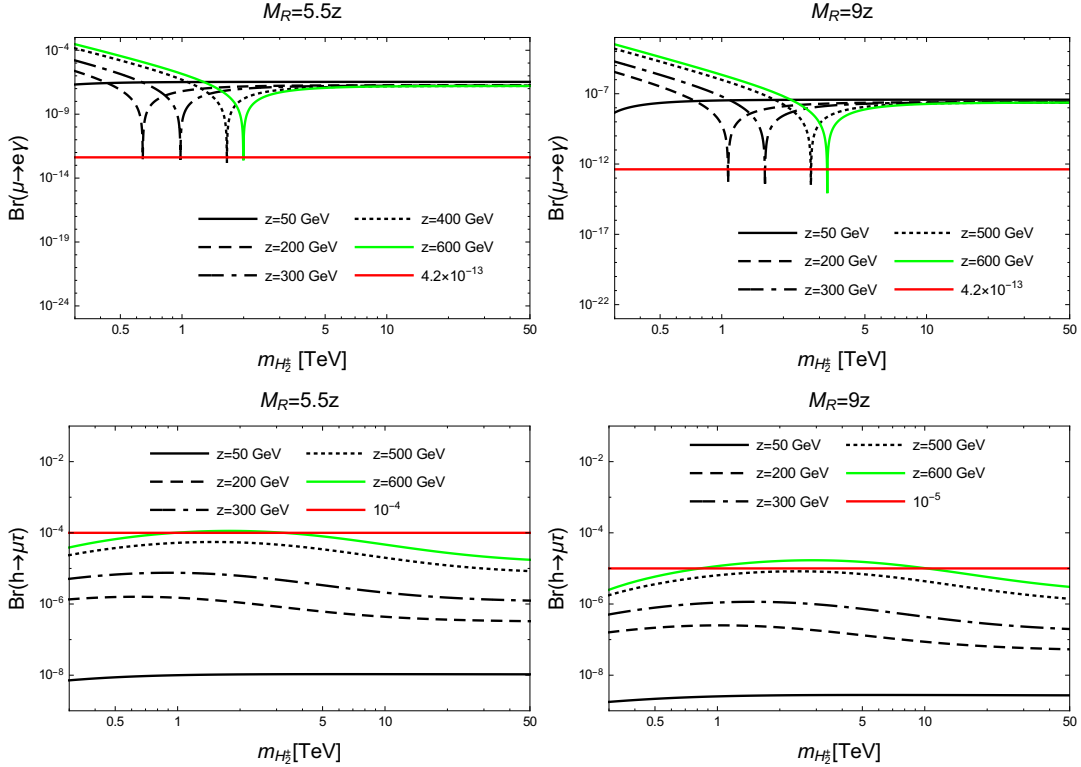


FIG. 3:  $\text{Br}(\mu \rightarrow e\gamma)$  (upper) and  $\text{Br}(h_1^0 \rightarrow \mu\tau)$  (lower) as functions of  $m_{H_2^\pm}$  with  $k = 5.5$  (left) and  $k = 9$  (right).

ruled out by the bound of  $\text{Br}(\mu \rightarrow e\gamma)$ , unless narrow parts where particular contributions

from charged Higgs and gauge bosons are destructive. This interesting property of the 331ISS was indicated previously in Ref. [9]. Furthermore, it predicts allowed regions giving large  $\text{Br}(h_1^0 \rightarrow \mu\tau)$ . In particular, the largest values can reach  $\mathcal{O}(10^{-4})$  when  $k = 5.5$  and  $z = 600$  GeV, which is very close to the perturbative limit. In general, illustrations in two Figs. 2 and 3 suggest that this Br enhances significantly with smaller  $k$  and larger  $z$ , but changes slowly with invariance of  $m_{H_2^\pm}$ . In contrast,  $m_{H_2^\pm}$  play very important role to create allowed regions predicting large LFVHD. The  $\text{Br}(\mu \rightarrow e\gamma)$  does not depend on  $m_{H_2^\pm}$  when it is large enough. Furthermore, the Br deduces with increasing  $k$  and it will below the experimental bound if  $k$  is large enough.

The allowed regions in Fig. 3 are shown more explicitly in Fig. 4, corresponding to  $k = 5.5$  and  $k = 9$ . Only regions giving large  $\text{Br}(h_1^0 \rightarrow \mu\tau)$  are mentioned. They are bounded

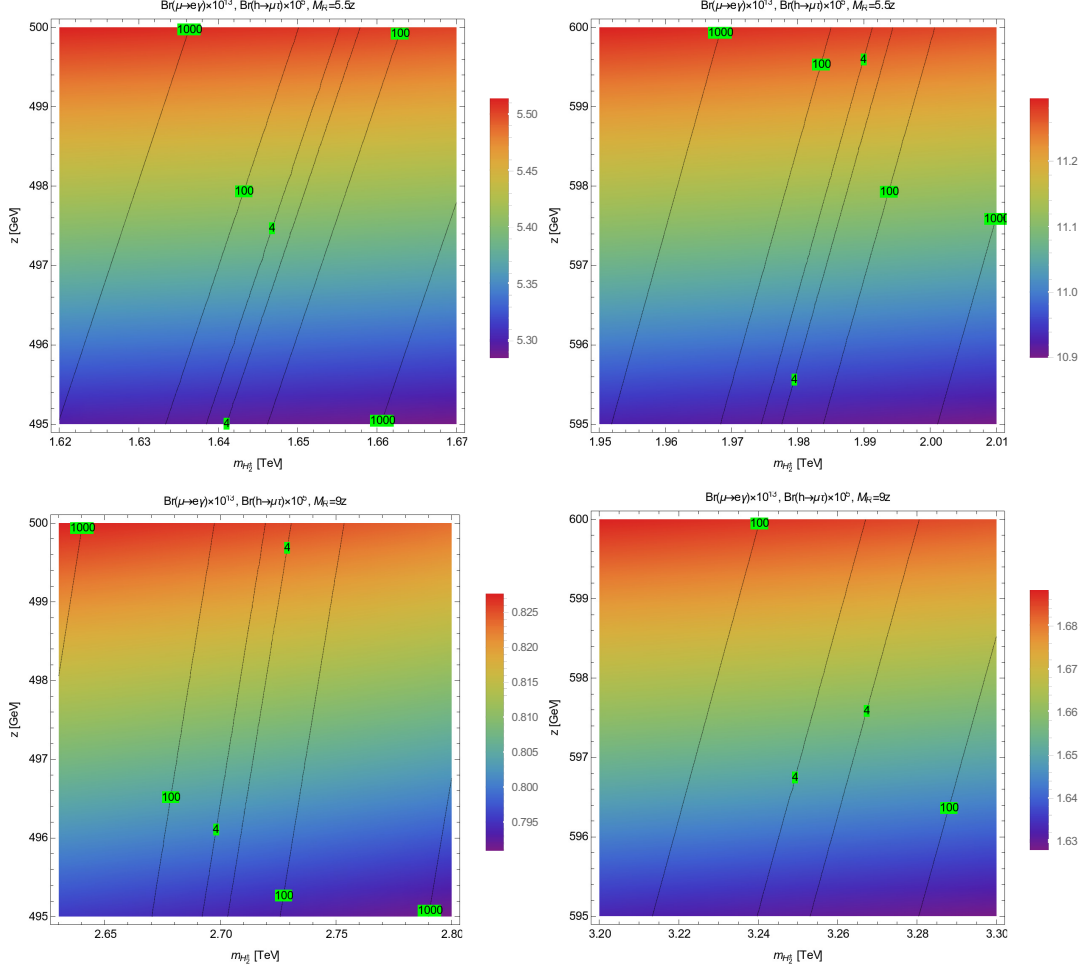


FIG. 4: Density plots of  $\text{Br}(h_1^0 \rightarrow \mu\tau)$  and contour plots of  $\text{Br}(\mu \rightarrow e\gamma)$  (black curves) as functions of  $m_{H_2^\pm}$  and  $z$ , with  $k = 5.5$  (upper) and  $k = 9$  (lower).

between two black curves presenting the constant value of  $\text{Br}(\mu \rightarrow e\gamma) \times 10^{13} = 4$ . Clearly,  $\text{Br}(h_1^0 \rightarrow \mu\tau)$  is sensitive with  $z$  and  $k$ , while changes slowly with changing values of  $m_{H_2^\pm}$ . In contrast, the suppressed  $\text{Br}(\mu \rightarrow e\gamma)$  allows narrow regions of the parameter space, where some certain relation of  $m_{H_2^\pm}$  with  $k$  and  $z$  is realized. Hence if these two channel decays are discovered by experiments, depending on the their specific values a relation between heavy neutrino and charged Higgs masses can be determined from the 331ISS frame work.

To understand how  $\text{Br}(h_1^0 \rightarrow \mu\tau)$  depends on the  $SU(3)_L$  breaking scale defined by  $m_Y$  in this work, four allowed regions corresponding four fixed values  $m_Y = 3, 4, 5$ , and 6 TeV are illustrated in Fig. 5. It can be seen that the Br of LFVHD depends weakly on the variance

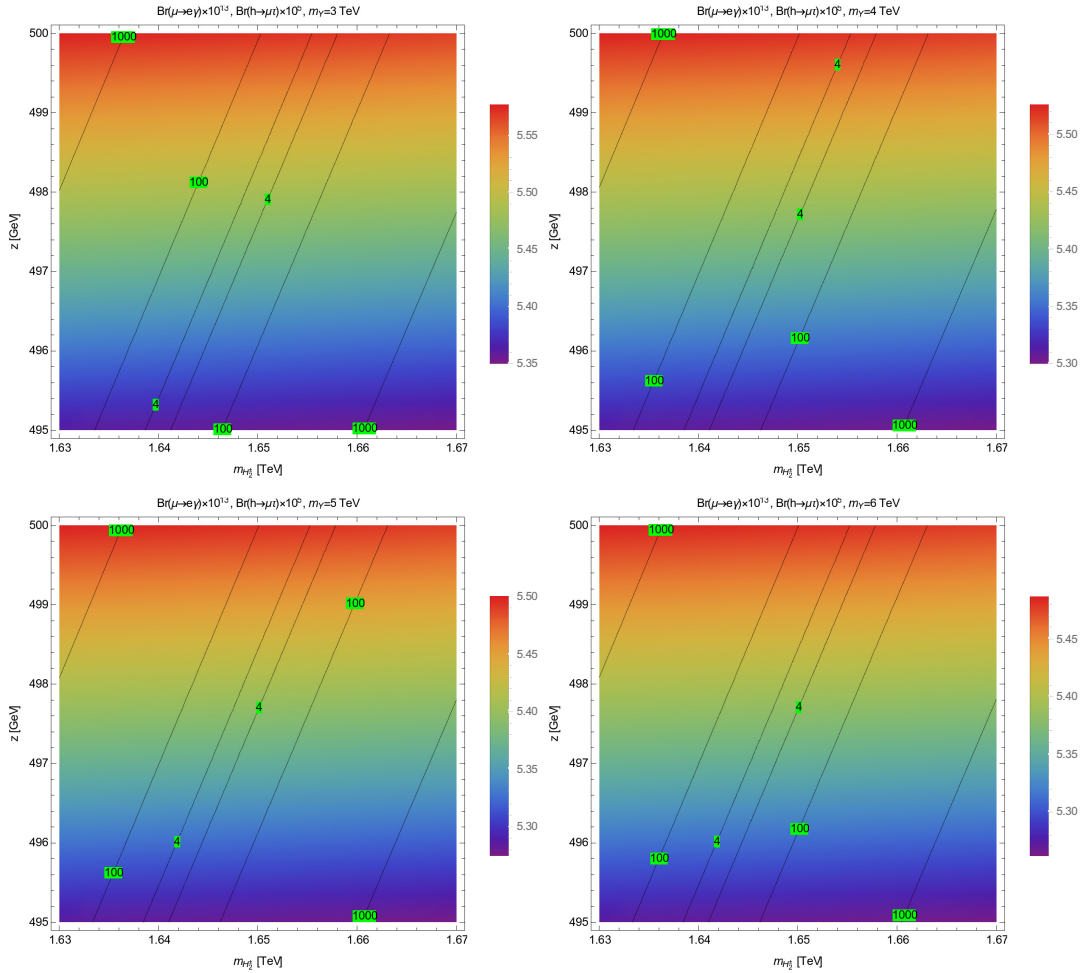


FIG. 5: Density plots of  $\text{Br}(h_1^0 \rightarrow \mu\tau)$  and contour plots of  $\text{Br}(\mu \rightarrow e\gamma)$  (black curves) as functions of  $m_{H_2^\pm}$  and  $z$ , with  $k = 5.5$ ,  $z$  around 500 GeV and different  $m_Y$ .

of  $m_Y$ , namely it decreases slowly with increasing  $m_Y$ . Hence, studies LFV decays will give useful information of heavy neutrinos and charged Higgs bosons besides phenomenology

caused by heavy gauge bosons discussed in many earlier works. More interestingly, the consequence may happen in large  $SU(3)_L$  scales which LHC cannot detect at present.

## V. CONCLUSION

The 331ISS models seem the most interesting among the well-known 331 models because of rich phenomenology indicated in many recent works. This work addressed a more attractive property, namely the LFVHD of the SM-like Higgs boson which are being searched at LHC. Assuming the absence of the tree level decays  $h_1^0 \rightarrow e_a e_b$  and  $e_j \rightarrow e_i \gamma$  ( $j > i$ ), the analytical formulas at one-loop level to calculate these decay rates in the 331ISS have been introduced. The divergent cancellation in the total decay amplitudes of  $h_1^0 \rightarrow e_a e_b$  was shown explicitly. From the numerical investigation, we have indicated that the  $\text{Br}(h_1^0 \rightarrow \mu\tau)$  predicted by the 331ISS can reach the large values of  $\mathcal{O}(10^{-5})$ . They are even very close to  $10^{-4}$ , for example in a special case of small  $k = 5.5$  and  $z \simeq 600$  GeV, close to the perturbative limit of the lepton Yukawa couplings. This value is larger than the one predicted from the simplest ISS version extended directly from the SM [18]. New charged Higgs bosons may give large contributions to both decay rates  $\text{Br}(\mu \rightarrow e\gamma)$  and  $\text{Br}(h_1^0 \rightarrow \mu\tau)$ , leading to the either constructive or destructive correlations with the ones from the charged gauge bosons. As a by product, recent experimental bound of  $\text{Br}(\mu \rightarrow e\gamma)$  rules out most of the regions of parameter space with small  $k$  and large  $z$ , except narrow regions arising from the destructive correlations between charged Higgs and gauge boson contributions. We have shown numerically that only these regions give large  $\text{Br}(h_1^0 \rightarrow \mu\tau) > 10^{-5}$  when  $400\text{GeV} < z < 600$  GeV and  $k \leq 9$  in the case of Majorana mass matrix  $M_R$  being proportional to the identity one. Furthermore, these large values of  $\text{Br}(h_1^0 \rightarrow \mu\tau)$  depend weakly on the heavy charged boson masses, but require the heavy neutrino mass scale  $M_R$  and  $m_{H_2^\pm}$  to be few TeV, which can be detected by the recent colliders. The  $\text{Br}(h_1^0 \rightarrow \tau e)$  has the same result. In conclusion, large branching ratios of the LFV processes like  $h_1^0 \rightarrow \mu\tau, e\tau$  will support the 331ISS and may rule out the original 331RHN containing small exotic neutrino masses. Additionally, many properties of heavy neutrinos and charged Higgs bosons in the 331ISS frame work may be determined independently with the  $SU(3)_L$  scale.

## Acknowledgments

This research is funded by Vietnam National Foundation for Science and Technology Development (NAFOSTED) under grant number 103.01-2015.33.

## Appendix A: Form factors of LFVHD in the unitary gauge

This Appendix listed all analytic formulas of one-loop contributions to LFVHD defined in Eq. (37). They are written in terms of Passarino-Veltman functions that were defined thoroughly in Refs. [6, 19]. Using the notations  $D_0 = k^2 - M_0^2 + i\delta$ ,  $D_1 = (k - p_1)^2 - M_1^2 + i\delta$  and  $D_2 = (k + p_2)^2 - M_2^2 + i\delta$ , where  $\delta$  is infinitesimally a positive real quantity, the one-loop integrals and Passarino-Veltman functions needed in this work are

$$\begin{aligned} B_{0,\mu}^{(i)} &\equiv \frac{(2\pi\mu)^{4-D}}{i\pi^2} \int \frac{d^D k \{1, k_\mu\}}{D_0 D_i}, \quad B_0^{(12)} \equiv \frac{(2\pi\mu)^{4-D}}{i\pi^2} \int \frac{d^D k}{D_1 D_2}, \\ C_{0,\mu} &\equiv C_{0,\mu}(M_0, M_1, M_2) = \frac{1}{i\pi^2} \int \frac{d^4 k \{1, k_\mu\}}{D_0 D_1 D_2}, \\ B_\mu^{(i)} &= B_1^{(i)} p_{i\mu}, \quad C_\mu = C_1 p_{1\mu} + C_2 p_{2\mu} \end{aligned}$$

where  $i = 1, 2$ . In addition,  $D = 4 - 2\epsilon \leq 4$  is the dimension of the integral;  $M_0, M_1, M_2$  are masses of virtual particles in the loop; and  $\mu$  is an arbitrary mass parameter introduced via dimensional regularization [32]. The external momenta of the final leptons shown in Fig. 1 satisfy  $p_1^2 = m_a^2$ ,  $p_2^2 = m_b^2$  and  $(p_1 + p_2)^2 = m_{h_1^0}^2$ , where  $m_{h_1^0}$  is the SM-like Higgs boson mass, and  $m_{a,b}$  are lepton masses. In the limit  $m_{a,b} \simeq 0$ , analytic formulas of  $B_{0,1}^{(i)}$ ,  $B_0^{(12)}$ ,  $C_0$  and  $C_{1,2}$  were shown in Refs. [6, 17, 19], hence we will not repeat here. These functions are used for our numerical investigation. We stress that they were checked numerically to be well consistent with the exact results computed by LoopTools [33], as concerned in Ref. [34].

The analytic expressions of  $\Delta_{L,R}^{(i)W} \equiv \Delta_{(ab)L,R}^{(i)W}$ , where  $i$  implies the diagram (i) in Fig. 1, are

$$\begin{aligned} \Delta_L^{(1)W} &= \frac{g^3 c_\alpha m_a}{64\pi^2 m_W^3} \sum_{i=1}^9 U_{ai}^{\nu*} U_{bi}^\nu \left\{ m_{n_i}^2 \left( B_1^{(1)} - B_0^{(1)} - B_0^{(2)} \right) - m_b^2 B_1^{(2)} + \left( 2m_W^2 + m_{h_1^0}^2 \right) m_{n_i}^2 C_0 \right. \\ &\quad \left. - \left[ 2m_W^2 (2m_W^2 + m_{n_i}^2 + m_a^2 - m_b^2) + m_{n_i}^2 m_{h_1^0}^2 \right] C_1 + \left[ 2m_W^2 (m_a^2 - m_{h_1^0}^2) + m_b^2 m_{h_1^0}^2 \right] C_2 \right\}, \\ \Delta_R^{(1)W} &= \frac{g^3 c_\alpha m_b}{64\pi^2 m_W^3} \sum_{i=1}^9 U_{ai}^{\nu*} U_{bi}^\nu \left\{ -m_{n_i}^2 \left( B_1^{(2)} + B_0^{(1)} + B_0^{(2)} \right) + m_a^2 B_1^{(1)} + \left( 2m_W^2 + m_{h_1^0}^2 \right) m_{n_i}^2 C_0 \right. \end{aligned}$$

$$\begin{aligned}
& - \left[ 2m_W^2 (m_b^2 - m_h^2) + m_a^2 m_{h_1^0}^2 \right] C_1 + \left[ 2m_W^2 (2m_W^2 + m_{n_i}^2 - m_a^2 + m_b^2) + m_{n_i}^2 m_{h_1^0}^2 \right] C_2 \Big\} , \\
\Delta_L^{(5)W} &= \frac{g^3 c_\alpha m_a}{64\pi^2 m_W^3} \sum_{i,j=1}^9 U_{ai}^{\nu*} U_{bj}^\nu \left\{ \lambda_{ij}^{0*} m_{n_j} \left[ B_0^{(12)} - m_W^2 C_0 + (2m_W^2 + m_{n_i}^2 - m_a^2) C_1 \right] \right. \\
& \quad \left. + \lambda_{ij}^0 m_{n_i} \left[ B_1^{(1)} + (2m_W^2 + m_{n_j}^2 - m_b^2) C_1 \right] \right\} , \\
\Delta_R^{(5)W} &= \frac{g^3 c_\alpha m_b}{64\pi^2 m_W^3} \sum_{i=1}^9 U_{ai}^{\nu*} U_{bj}^\nu \left\{ \lambda_{ij}^0 m_{n_i} \left[ B_0^{(12)} - m_W^2 C_0 - (2m_W^2 + m_{n_j}^2 - m_b^2) C_2 \right] \right. \\
& \quad \left. - \lambda_{ij}^{0*} m_{n_j} \left[ B_1^{(2)} + (2m_W^2 + m_{n_i}^2 - m_a^2) C_2 \right] \right\} , \\
\Delta_L^{(7+8)W} &= \frac{g^3 m_a m_b^2 c_\alpha}{64\pi^2 m_W^3 (m_a^2 - m_b^2)} \sum_{i=1}^9 U_{ai}^{\nu*} U_{bi}^\nu \left[ 2m_{n_i}^2 (B_0^{(1)} - B_0^{(2)}) \right. \\
& \quad \left. - (2m_W^2 + m_{n_i}^2) (B_1^{(1)} + B_1^{(2)}) - m_a^2 B_1^{(1)} - m_b^2 B_2^{(1)} \right] , \\
\Delta_R^{(7+8)W} &= \frac{m_a}{m_b} \Delta_L^{(7+8)W} . \tag{A1}
\end{aligned}$$

Defining  $\Delta_{L,R}^{(i)Y} = \Delta_{(ab)L,R}^{(i)YH_1^\pm} + \Delta_{(ab)L,R}^{(i)YH_2^\pm}$  with  $i = 4, 6, 9, 10$ , the analytic expressions of  $\Delta_{L,R}^{(i)Y} \equiv \Delta_{(ab)L,R}^{(i)Y}$  are

$$\begin{aligned}
\Delta_L^{(1)Y} &= -\frac{g^3 m_a (\sqrt{2}s_\alpha c_\theta - c_\alpha s_\theta)}{64\sqrt{2}\pi^2 m_Y^3} \sum_{i=1}^9 U_{(a+3)i}^{\nu*} U_{(b+3)i}^\nu \left\{ m_{n_i}^2 (B_1^{(1)} - B_0^{(1)} - B_0^{(2)}) - m_b^2 B_1^{(2)} \right. \\
& \quad + (2m_Y^2 + m_{h_1^0}^2) m_{n_i}^2 C_0 - \left[ 2m_Y^2 (2m_Y^2 + m_{n_i}^2 + m_a^2 - m_b^2) + m_{n_i}^2 m_{h_1^0}^2 \right] C_1 \\
& \quad \left. + \left[ 2m_Y^2 (m_a^2 - m_{h_1^0}^2) + m_b^2 m_{h_1^0}^2 \right] C_2 \right\} , \\
\Delta_R^{(1)Y} &= -\frac{g^3 m_b (\sqrt{2}s_\alpha c_\theta - c_\alpha s_\theta)}{64\sqrt{2}\pi^2 m_Y^3} \sum_{i=1}^9 U_{(a+3)i}^{\nu*} U_{(b+3)i}^\nu \left\{ -m_{n_i}^2 (B_1^{(2)} + B_0^{(1)} + B_0^{(2)}) + m_a^2 B_1^{(1)} \right. \\
& \quad + (2m_Y^2 + m_{h_1^0}^2) m_{n_i}^2 C_0 - \left[ 2m_Y^2 (m_b^2 - m_{h_1^0}^2) + m_a^2 m_{h_1^0}^2 \right] C_1 \\
& \quad \left. + \left[ 2m_Y^2 (2m_Y^2 + m_{n_i}^2 - m_a^2 + m_b^2) + m_{n_i}^2 m_{h_1^0}^2 \right] C_2 \right\} , \\
\Delta_L^{(2)Y} &= \frac{g^3 m_a c_\theta (c_\alpha c_\theta + \sqrt{2}s_\alpha s_\theta)}{64\pi^2 m_W m_Y^2} \sum_{i=1}^9 U_{(a+3)i}^{\nu*} \\
& \quad \times \left\{ \lambda_{bi}^{L,1} m_{n_i} \left[ B_0^{(1)} - B_1^{(1)} + (m_Y^2 + m_{H_1^\pm}^2 - m_{h_1^0}^2) C_0 + (m_Y^2 - m_{H_1^\pm}^2 + m_{h_1^0}^2) C_1 \right] \right. \\
& \quad \left. + \lambda_{bi}^{R,1} m_b \left[ 2m_Y^2 C_1 - (m_Y^2 + m_{H_1^\pm}^2 - m_{h_1^0}^2) C_2 \right] \right\} , \\
\Delta_R^{(2)Y} &= \frac{g^3 c_\theta (c_\alpha c_\theta + \sqrt{2}s_\alpha s_\theta)}{64\pi^2 m_W m_Y^2} \sum_{i=1}^9 U_{(a+3)i}^{\nu*} \\
& \quad \times \left\{ \lambda_{bi}^{L,1} m_b m_{n_i} \left[ -2m_Y^2 C_0 - (m_Y^2 - m_{H_1^\pm}^2 + m_{h_1^0}^2) C_2 \right] \right. \\
& \quad \left. + \lambda_{bi}^{R,1} \left[ -m_{n_i}^2 B_0^{(1)} + m_a^2 B_1^{(1)} + m_{n_i}^2 (m_Y^2 - m_{H_1^\pm}^2 + m_{h_1^0}^2) C_0 \right] \right\}
\end{aligned}$$

$$\begin{aligned}
& + \left[ 2m_Y^2 \left( m_{h_1^0}^2 - m_b^2 \right) - m_a^2 \left( m_Y^2 - m_{H_1^\pm}^2 + m_{h_1^0}^2 \right) \right] C_1 + 2m_b^2 m_Y^2 C_2 \Big] \Big\} , \\
\Delta_L^{(3)Y} &= \frac{g^3 c_\theta (c_\alpha c_\theta + \sqrt{2} s_\alpha s_\theta)}{64\pi^2 m_W m_Y^2} \sum_{i=1}^9 U_{(b+3)i}^\nu \\
& \times \left\{ \lambda_{ai}^{L,1*} m_a m_{n_i} \left[ -2m_Y^2 C_0 + \left( m_Y^2 - m_{H_1^\pm}^2 + m_{h_1^0}^2 \right) C_1 \right] \right. \\
& + \lambda_{ai}^{R,1*} \left[ -m_{n_i}^2 B_0^{(2)} - m_b^2 B_1^{(2)} + m_{n_i}^2 \left( m_Y^2 - m_{H_1^\pm}^2 + m_{h_1^0}^2 \right) C_0 \right. \\
& \left. \left. - 2m_a^2 m_Y^2 C_1 - \left[ 2m_Y^2 \left( m_{h_1^0}^2 - m_a^2 \right) - m_b^2 \left( m_Y^2 - m_{H_1^\pm}^2 + m_{h_1^0}^2 \right) \right] C_2 \right] \right\} , \\
\Delta_R^{(3)Y} &= \frac{g^3 m_b c_\theta (c_\alpha c_\theta + \sqrt{2} s_\alpha s_\theta)}{64\pi^2 m_W m_Y^2} \sum_{i=1}^9 U_{(b+3)i}^\nu \\
& \times \left\{ \lambda_{ai}^{L,1*} m_{n_i} \left[ B_0^{(2)} + B_1^{(2)} \right. \right. \\
& + \left( m_Y^2 + m_{H_1^\pm}^2 - m_{h_1^0}^2 \right) C_0 - \left( m_Y^2 - m_{H_1^\pm}^2 + m_{h_1^0}^2 \right) C_2 \Big] \\
& \left. + \lambda_{ai}^{R,1*} m_a \left[ \left( m_Y^2 + m_{H_1^\pm}^2 - m_{h_1^0}^2 \right) C_1 - 2m_Y^2 C_2 \right] \right\} , \\
\Delta_L^{(4)YH_k^\pm} &= \frac{g^2 \lambda_{H_k}^\pm f_k}{16\pi^2 m_W^2} \sum_{i=1}^9 \left[ -\lambda_{ai}^{R,k*} \lambda_{bi}^{L,k} m_{n_i} C_0 - \lambda_{ai}^{L,k*} \lambda_{bi}^{L,k} m_a C_1 + \lambda_{ai}^{R,k*} \lambda_{bi}^{R,k} m_b C_2 \right] , \\
\Delta_R^{(4)YH_k^\pm} &= \frac{g^2 \lambda_{H_k}^\pm f_k}{16\pi^2 m_W^2} \sum_{i=1}^9 \left[ -\lambda_{ai}^{L,k*} \lambda_{bi}^{R,k} m_{n_i} C_0 - \lambda_{ai}^{R,k*} \lambda_{bi}^{R,k} m_a C_1 + \lambda_{ai}^{L,k*} \lambda_{bi}^{L,k} m_b C_2 \right] , \\
\Delta_L^{(5)Y} &= \frac{g^3 c_\alpha m_a}{64\pi^2 m_W m_Y^2} \\
& \times \sum_{i,j=1}^9 U_{(a+3)i}^{\nu*} U_{(b+3)j}^\nu \left\{ \lambda_{ij}^{0*} m_{n_j} \left[ B_0^{(12)} - m_Y^2 C_0 + (2m_Y^2 + m_{n_i}^2 - m_a^2) C_1 \right] \right. \\
& \left. + \lambda_{ij}^0 m_{n_i} \left[ B_1^{(1)} + (2m_Y^2 + m_{n_j}^2 - m_b^2) C_1 \right] \right\} , \\
\Delta_R^{(5)Y} &= \frac{g^3 c_\alpha m_b}{64\pi^2 m_W m_Y^2} \\
& \times \sum_{i,j=1}^9 U_{(a+3)i}^{\nu*} U_{(b+3)j}^\nu \left\{ \lambda_{ij}^{0*} m_{n_i} \left[ B_0^{(12)} - m_Y^2 C_0 - (2m_Y^2 + m_{n_j}^2 - m_b^2) C_2 \right] \right. \\
& \left. - \lambda_{ij}^{0*} m_{n_j} \left[ B_1^{(2)} + (2m_Y^2 + m_{n_i}^2 - m_a^2) C_2 \right] \right\} , \\
\Delta_L^{(6)YH_k^\pm} &= -\frac{g^3 c_\alpha f_k}{32\pi^2 m_W^3} \sum_{i,j=1}^9 \left\{ \lambda_{ij}^{0*} \left[ \lambda_{ai}^{R,k*} \lambda_{bj}^{L,k} \left( B_0^{(12)} + m_{H_k^\pm}^2 C_0 - m_a^2 C_1 + m_b^2 C_2 \right) \right. \right. \\
& + \lambda_{ai}^{R,k*} \lambda_{bj}^{R,k} m_b m_{n_j} C_2 - \lambda_{ai}^{L,k*} \lambda_{bj}^{L,k} m_a m_{n_i} C_1 \Big] \\
& + \lambda_{ij}^0 \left[ \lambda_{ai}^{R,k*} \lambda_{bj}^{L,k} m_{n_i} m_{n_j} C_0 + \lambda_{ai}^{R,k*} \lambda_{bj}^{R,k} m_{n_i} m_b (C_0 + C_2) \right. \\
& \left. \left. + \lambda_{ai}^{L,k*} \lambda_{bj}^{L,k} m_a m_{n_j} (C_0 - C_1) + \lambda_{ai}^{L,k*} \lambda_{bj}^{R,k} m_a m_b (C_0 - C_1 + C_2) \right] \right\} ,
\end{aligned}$$



$$\begin{aligned}
\Delta_R^{(6)YH_k^\pm} &= -\frac{g^3 c_\alpha f_k}{32\pi^2 m_W^3} \sum_{i,j=1}^9 \left\{ \lambda_{ij}^0 \left[ \lambda_{ai}^{L,k*} \lambda_{bj}^{R,k} \left( B_0^{(12)} + m_{H_k^\pm}^2 C_0 - m_a^2 C_1 + m_b^2 C_2 \right) \right. \right. \\
&\quad + \lambda_{ai}^{L,k*} \lambda_{bj}^{L,k} m_b m_{n_j} C_2 - \lambda_{ai}^{R,k*} \lambda_{bj}^{R,k} m_a m_{n_i} C_1 \left. \right] \\
&\quad + \lambda_{ij}^{0*} \left[ \lambda_{ai}^{L,k*} \lambda_{bj}^{R,k} m_{n_i} m_{n_j} C_0 + \lambda_{ai}^{L,k*} \lambda_{bj}^{L,k} m_{n_i} m_b (C_0 + C_2) \right. \\
&\quad + \lambda_{ai}^{R,k*} \lambda_{bj}^{R,k} m_a m_{n_j} (C_0 - C_1) + \lambda_{ai}^{R,k*} \lambda_{bj}^{L,k} m_a m_b (C_0 - C_1 + C_2) \left. \right] \left. \right\}, \\
\Delta_L^{(7+8)Y} &= \frac{g^3 m_a m_b^2 c_\alpha}{64\pi^2 m_W m_Y^2 (m_a^2 - m_b^2)} \sum_{i=1}^9 U_{(a+3)i}^{\nu*} U_{(b+3)i}^\nu \\
&\quad \times \left[ 2m_{n_i}^2 \left( B_0^{(1)} - B_0^{(2)} \right) - (2m_Y^2 + m_{n_i}^2) \left( B_1^{(1)} + B_1^{(2)} \right) - m_a^2 B_1^{(1)} - m_b^2 B_1^{(2)} \right], \\
\Delta_R^{(7+8)Y} &= \frac{m_a}{m_b} \Delta_L^{(7+8)Y}, \\
\Delta_L^{(9+10)YH_k^\pm} &= -\frac{g^3 c_\alpha f_k}{32\pi^2 m_W^3 (m_a^2 - m_b^2)} \\
&\quad \times \sum_{i=1}^9 \left[ m_a m_b m_{n_i} \lambda_{ai}^{L,k*} \lambda_{bi}^{R,k} \left( B_0^{(1)} - B_0^{(2)} \right) + m_{n_i} \lambda_{ai}^{R,k*} \lambda_{bi}^{L,k} \left( m_b^2 B_0^{(1)} - m_a^2 B_0^{(2)} \right) \right. \\
&\quad + m_a m_b \left( \lambda_{ai}^{L,k*} \lambda_{bi}^{L,k} m_b + \lambda_{ai}^{R,k*} \lambda_{bi}^{R,k} m_a \right) \left( B_1^{(1)} + B_1^{(2)} \right) \left. \right], \\
\Delta_R^{(9+10)YH_k^\pm} &= -\frac{g^3 c_\alpha f_k}{32\pi^2 m_W^3 (m_a^2 - m_b^2)} \\
&\quad \times \sum_{i=1}^9 \left[ m_a m_b m_{n_i} \lambda_{ai}^{R,k*} \lambda_{bi}^{L,k} \left( B_0^{(1)} - B_0^{(2)} \right) + m_{n_i} \lambda_{ai}^{L,k*} \lambda_{bi}^{R,k} \left( m_b^2 B_0^{(1)} - m_a^2 B_0^{(2)} \right) \right. \\
&\quad + m_a m_b \left( \lambda_{ai}^{R,k*} \lambda_{bi}^{R,k} m_b + \lambda_{ai}^{L,k*} \lambda_{bi}^{L,k} m_a \right) \left( B_1^{(1)} + B_1^{(2)} \right) \left. \right], \tag{A2}
\end{aligned}$$

where  $f_1 = c_\theta^2$  and  $f_2 = 1/2$ . The details to derive expressions in (A2) are the same as those shown in Refs. [6, 19], hence we do not present in this work. We note that the scalar functions  $\Delta_{L,R}^{(1)W}$  and  $\Delta_{L,R}^{(1,2,3)Y}$  include parts that do not depend on  $m_{n_i}$ , therefore vanish because of the GIM mechanism. They are ignored in (A1) and (A2).

The divergent cancellation in the total  $\Delta_{L,R}$  is shown as follows. The divergent parts contain in only  $B$ -functions:  $\text{div} B_0^{(1)} = \text{div} B_0^{(2)} = \text{div} B_0^{(12)} = 2\text{div} B_1^{(1)} = -2\text{div} B_1^{(2)} = \Delta_\epsilon$ . Ignoring the common factor of  $g^3/(64\pi^2 m_W^3)$  and using  $1/m_Y = \sqrt{2}s_\theta/m_W$ , the divergent parts of  $\Delta_L$  derived from (A2) are

$$\begin{aligned}
\text{div} \left[ \Delta_L^{(1)W} \right] &= m_a \Delta_\epsilon \times \left( -\frac{3c_\alpha}{2} \right) \sum_{i=1}^9 U_{ai}^{\nu*} U_{bi}^\nu m_{n_i}^2, \\
\text{div} \left[ \Delta_L^{(5)W} \right] &= m_a \Delta_\epsilon \times c_\alpha \sum_{i,j=1}^9 U_{ai}^{\nu*} U_{bj}^\nu \left( \lambda_{ij}^{0*} m_{n_j} + \frac{1}{2} \lambda_{ij}^0 m_{n_i} \right),
\end{aligned}$$

$$\begin{aligned}
\text{div} \left[ \Delta_L^{(7+8)W} \right] &= \text{div} \left[ \Delta_L^{(4)Y} \right] = \text{div} \left[ \Delta_L^{(7+8)Y} \right] = 0, \\
\text{div} \left[ \Delta_L^{(1)Y} \right] &= m_a \Delta_\epsilon \times 3s_\theta^3 \left( \sqrt{2}s_\alpha c_\theta - c_\alpha s_\theta \right) \sum_{i=1}^9 U_{(a+3)i}^{\nu*} U_{(b+3)i}^\nu m_{n_i}^2, \\
\text{div} \left[ \Delta_L^{(2)Y} \right] &= m_a \Delta_\epsilon \times s_\theta^2 c_\theta \left( c_\alpha c_\theta + \sqrt{2}s_\alpha s_\theta \right) \sum_{i=1}^9 U_{(a+3)i}^{\nu*} \lambda_{bi}^{L,1} m_{n_i}, \\
\text{div} \left[ \Delta_L^{(3)Y} \right] &= m_a \Delta_\epsilon \times \left[ -2s_\theta^2 c_\theta \left( c_\alpha c_\theta + \sqrt{2}s_\alpha s_\theta \right) \right] \sum_{i=1}^9 U_{(a+3)i}^{\nu*} U_{(b+3)i}^\nu m_{n_i}^2, \\
\text{div} \left[ \Delta_L^{(5)Y} \right] &= m_a \Delta_\epsilon \times 2s_\theta^2 c_\alpha \sum_{i,j=1}^9 U_{(a+3)i}^{\nu*} U_{(b+3)j}^\nu \left( \lambda_{ij}^{0*} m_{n_j} + \frac{1}{2} \lambda_{ij}^0 m_{n_i} \right), \\
\text{div} \left[ \Delta_L^{(6)YH_1^\pm} \right] &= m_a \Delta_\epsilon \times (-2c_\alpha c_\theta^2) \sum_{i,j=1}^9 U_{(a+3)i}^{\nu*} \lambda_{ij}^{0*} \lambda_{bj}^{L,1}, \\
\text{div} \left[ \Delta_L^{(6)YH_2^\pm} \right] &= m_a \Delta_\epsilon \times (-c_\alpha) \sum_{i,j=1}^9 U_{ai}^{\nu*} \lambda_{ij}^{0*} \lambda_{bj}^{L,2}, \\
\text{div} \left[ \Delta_L^{(9+10)YH_1^\pm} \right] &= m_a \Delta_\epsilon \times (2c_\alpha c_\theta^2) \sum_{i=1}^9 U_{(a+3)i}^{\nu*} \lambda_{bi}^{L,1} m_{n_i}, \\
\text{div} \left[ \Delta_L^{(9+10)YH_2^\pm} \right] &= m_a \Delta_\epsilon \times c_\alpha \sum_{i=1}^9 U_{ai}^{\nu*} \lambda_{bi}^{L,2} m_{n_i}, \tag{A3}
\end{aligned}$$

Using equalities  $M^\nu = U^{\nu*} \hat{M}^\nu U^{\nu\dagger}$  and (38), we can prove that

$$\begin{aligned}
\text{div} \left[ \Delta_{L,R}^{(1)W} \right] &\sim \sum_{i=1}^9 U_{ai}^{\nu*} U_{bi}^\nu m_{n_i}^2 = \left[ U^\nu (\hat{M}^\nu)^2 U^{\nu\dagger} \right]_{ba} = (m_D^* m_D^T)_{ba} \\
&= (m_D^\dagger m_D)_{ba}, \\
\text{div} \left[ \Delta_{L,R}^{(5)W} \right] &\sim \sum_{i,j=1}^9 U_{ai}^{\nu*} U_{bj}^\nu \lambda_{ij}^{0*} m_{n_j}, \sum_{i,j=1}^9 U_{ai}^{\nu*} U_{bj}^\nu \lambda_{ij}^0 m_{n_i} = (m_D^* m_D^T)_{ba} \\
&= (m_D^\dagger m_D)_{ba}, \\
\text{div} \left[ \Delta_{L,R}^{(1,3)Y} \right] &\sim \sum_{i=1}^9 U_{(a+3)i}^{\nu*} U_{(b+3)i}^\nu m_{n_i}^2 = \left[ U^\nu (\hat{M}^\nu)^2 U^{\nu\dagger} \right]_{(b+3)(a+3)} \\
&= (m_D^\dagger m_D + M_R^* M_R^T)_{ba}, \\
\text{div} \left[ \Delta_{L,R}^{(2)Y, (9+10)YH_1^\pm} \right] &\sim \sum_{i=1}^9 U_{(a+3)i}^{\nu*} \lambda_{bi}^{L,1} m_{n_i} = (m_D^* m_D)_{ba} + t_\theta^2 (M_R^* M_R^T)_{ba} \\
&= -(m_D^\dagger m_D)_{ba} + t_\theta^2 (M_R^* M_R^T)_{ba}, \\
\text{div} \left[ \Delta_{L,R}^{(5)Y} \right] &\sim \sum_{i,j=1}^9 U_{(a+3)i}^{\nu*} U_{(b+3)j}^\nu \lambda_{ij}^{0*} m_{n_j}, \sum_{i,j=1}^9 U_{(a+3)i}^{\nu*} U_{(b+3)j}^\nu \lambda_{ij}^0 m_{n_i}
\end{aligned}$$

$$\begin{aligned}
& \sim (m_D^\dagger m_D)_{ba} - \sqrt{2}t_\alpha t_\theta (M_R^* M_R^T)_{ba}, \\
\text{div} \left[ \Delta_{L,R}^{(6)YH_1^\pm} \right] & \sim \sum_{i,j=1}^9 U_{(a+3)i}^{\nu*} \lambda_{ij}^{0*} \lambda_{bj}^{L,1} = (m_D^* m_D)_{ba} - \sqrt{2}t_\alpha t_\theta^3 (M_R^* M_R^T)_{ba} \\
& = -(m_D^\dagger m_D)_{ba} - \sqrt{2}t_\alpha t_\theta^3 (M_R^* M_R^T)_{ba}, \\
\text{div} \left[ \Delta_{L,R}^{(6)YH_2^\pm} \right] & \sim \sum_{i,j=1}^9 U_{ai}^{\nu*} \lambda_{ij}^{0*} \lambda_{bj}^{L,2} = -(m_D^\dagger m_D)_{ba}, \\
\text{div} \left[ \Delta_{L,R}^{(9+10)YH_2^\pm} \right] & \sim \sum_{i=1}^9 U_{ai}^{\nu*} \lambda_{bi}^{L,2} m_{ni} = -(m_D^\dagger m_D)_{ba}, \tag{A4}
\end{aligned}$$

where we have used the antisymmetric property of  $m_D$ :  $m_D^T = -m_D$ . From this, it can be seen that  $\text{div} \left[ \Delta_L^{(1)W} \right] + \text{div} \left[ \Delta_L^{(5)W} \right] = \text{div} \left[ \Delta_L^{(6)YH_2^\pm} \right] + \text{div} \left[ \Delta_L^{(9+10)YH_2^\pm} \right] = 0$ . Sum of the remaining divergent parts is :

$$\begin{aligned}
& \text{div} \left[ \Delta_L^{(1+2+3+5)Y} + \Delta_L^{(6+9+10)YH_1^\pm} \right] \\
& \sim (m_D^\dagger m_D)_{ba} \left\{ \sqrt{2}s_\alpha s_\theta^2 c_\theta (3 - 1 - 2) + c_\alpha \left[ s_\theta^2 (-3s_\theta^2 - c_\theta^2 - 2c_\theta^2 + 3) + 2s_\theta^2 - 2s_\theta^2 \right] \right\} \\
& + (M_R^* M_R^T)_{ba} \left[ \sqrt{2}s_\alpha \frac{s_\theta^2}{c_\theta} (3c_\theta^2 + s_\theta^2 - 2c_\theta^2 - 3 + 2) + c_\alpha s_\theta^2 (-3s_\theta^2 + s_\theta^2 - 2c_\theta^2 + 2) \right] \\
& = 0. \tag{A5}
\end{aligned}$$

Finally, the proof of divergent cancellation in  $\Delta_R$  are exactly the same as that in  $\Delta_L$ .

- 
- [1] CMS Collaboration, Phys.Lett. **B 749**, 337 (2015); Phys. Lett. **B 763**, 472 (2016); ATLAS Collaboration, JHEP 11 (2015) 211; Eur. Phys. J. C 77 (2017) 70; CMS Collaboration, "Search for lepton flavour violating decays of the Higgs boson to  $\mu\tau$  and  $e\tau$  in proton-proton collisions at  $\sqrt{s} = 13 \text{ TeV}$ ", arXiv:1712.07173 [hep-ex].
  - [2] ATLAS Collaboration, Phys. Lett. B 716, 1 (2012); CMS Collaboration, Phys. Lett. B 716, 30 (2012); CMS Collaboration, JHEP 06, 081 (2013).
  - [3] S. Kanemura, K. Matsuda, T. Ota, T. Shindou, E. Takasugi and K.Tsumura, Phys. Lett. B 599, 83 (2004); S. Davidson and P. Verrier, Phys. Rev. D 86, 111701 (2012); S. Bressler, A. Dery and A. Efrati, Phys. Rev. D 90, 015025 (2014); D. A. Sierra and A. Vicente, Phys. Rev. D 90, 115004 (2014); C. X. Yue, C. Pang and Y. C. Guo, J. Phys. G 42, 075003 (2015); S. Banerjee, B. Bhattacharjee, M. Mitra, M. Spannowsky, JHEP 1607, 059 (2016); I. Chakraborty, A.

- Datta, A. Kundu, J.Phys. G43, 125001 (2016); Q. Qin, Q. Li, C.D Lu, F.S Yu, S.H Zhou, " *Charged lepton flavor violating Higgs decays at the CEPC*", arXiv:1711.07243 [hep-ph].
- [4] G. Blankenburg, J. Ellis and G. Isidori, Phys. Lett. B 712, 386 (2012); J. H. Garcia, N. Riush and A. Santamaria, JHEP 1611, 084 (2016).
- [5] A. Pilaftsis, Phys.Lett. B285, 68 (1992); J. G. Korner, A. Pilaftsis, K. Schilcher, Phys. Rev. D 47, 1080 (1993); A. Pilaftsis, Z.Phys. C55, 275 (1992); A. Ilakovac, Phys.Rev. D62, 036010 (2000); J.L. Diaz-Cruz, J.J. Toscano, Phys.Rev. D 62, 116005 (2000); X. G. He, J.Tandean, Y. J. Zheng, JHEP 1509, 093 (2015); W. Altmannshofer, S. Gori, A. L. Kagan, L. Silvestrini, J. Zupan, Phys. Rev. D 93, 031301 (2016); I. Dorsner, S. Fajfer, A. Greljo, J. F. Kamenik, N. Kosnik, Ivan Nisandzic, JHEP 1506, 108 (2015); R. Harnik, J. Kopp and J. Zupan, JHEP 1303, 026 (2013); A. Celis, V. Cirigliano and E. Passemar, Phys. Rev. D 89, 013008 (2014); A. Dery, A. Efrati, Y. Nir, Y. Soreq and V. Susi, Phys. Rev. D 90, 115022 (2014); J. Heeck, M. Holthausen, W. Rodejohann and Y. Shimizu, Nucl. Phys. B 896, 281 (2015); A. Crivellin, G. D'Ambrosio and J. Heeck, Phys. Rev. D 91, 075006 (2015); L. D. Lima, C. S. Machado, R. D. Matheus, L. A. F. D. Prado, JHEP 1511, 074 (2015); I. d. M. Varzielas, O. Fischer, V. Maurer, JHEP 1508, 080 (2015); C. F. Chang, C. H. V. Chang, C. S. Nugroho, T. C. Yuan, Nucl.Phys. B910, 293 (2016); C. H. Chen, T. Nomura, Eur.Phys.J. C76, 353 (2016); K. Huitu, V. Keus, N. Koivunen, O. Lebedev, JHEP 1605, 026 (2016); K. Cheung, W. Y. Keung, P. Y. Tseng, Phys. Rev. D 93, 015010 (2016); A. Crivellin, G. D'Ambrosio, J. Heeck, Phys. Rev. Lett. 114, 151801 (2015); N. Bizot, S. Davidson, M. Frigerio, J. L. Kneur, JHEP 1603, 073 (2016); M. Sher, K. Thrasher, Phys. Rev. D 93, 055021 (2016); M. Aoki, S. Kanemura, K. Sakurai, H. Sugiyama, Phys.Lett. B763, 352 (2016); H.K. Guo, Y.Y. Li, T. Liu, M. R. Musolf, J. Shu, Phys.Rev. D96, 115034 (2017) ; P.S. Bhupal Dev, R. Franceschini, R.N. Mohapatra, Phys.Rev. D86, 093010 (2012); J. H. Garcia, T. Ohlsson, S. Riad, J. Wiren, JHEP 1704, 130 (2017); B. Yang, J. Han, N. Liu, Phys.Rev. D95, 035010 (2017); A. Lami, P. Roig, Phys.Rev. D94, 056001 (2016).
- [6] L.T. Hue, H.N. Long, T.T. Thuc, T. Phong Nguyen, Nucl.Phys. B907, 37 (2016); T.T. Thuc, L.T. Hue, H.N. Long, and T. Phong Nguyen, Phys.Rev. D93, 115026 (2016).
- [7] A. Brignole, A. Rossi, Phys. Lett. B 566, 217 (2003); A. Brignole, A. Rossi, Nucl. Phys. B 701, 53 (2004); E. Arganda, A. M. Curiel, M. J. Herrero, D. Temes, Phys.Rev. D71, 035011 (2005); M. A. Catania, E. Arganda, M. J. Herrero, JHEP 1309, 160 (2013); JHEP 1510, 192

- (2015); E. Arganda, M. J. Herrero, X. Marcano, C. Weiland, Phys. Rev. D 93, 055010 (2016); P. T. Giang, L. T. Hue, D. T. Huong, and H. N. Long, Nucl. Phys. B 864, 85 (2012); D. T. Binh, L. T. Hue, D. T. Huong, H. N. Long, Eur. Phys. J. C 74, 2851 (2014); E. Arganda, M. J. Herrero, R. Morales and A. Szykman, JHEP 1603, 055 (2016); J. L. Diaz-Cruz, JHEP 0305, 036 (2003); S. Baek, Z.F. Kang, JHEP 1603, 106 (2016); S. Baek, K. Nishiwaki, Phys. Rev. D 93, 015002 (2016); H.B. Zhang, T.F. Feng, S.M. Zhao, Y.L. Yan, Chin.Phys. C41, 043106 (2017).
- [8] MEG Collaboration, Eur.Phys.J. C76, 434 (2016).
- [9] S. M. Boucenna, Jose W. F. Valle, A. Vicente, Phys.Rev. D92, 053001 (2015).
- [10] G. Arcadi, C.P. Ferreira, F. Goertz, M.M. Guzzo, F. S. Queiroz, A.C.O. Santos, "*Lepton Flavor Violation Induced by Dark Matter*", arXiv:1712.02373 [hep-ph].
- [11] M. Lindner, M. Platscher, F. S. Queiroz, Phys.Rep. (2018), arXiv:1610.06587 [hep-ph].
- [12] L.T. Hue, L.D. Ninh, T.T. Thuc, N.T.T. Dat, *Exact one-loop results for  $l_i \rightarrow l_j \gamma$  in 3-3-1 models*, arXiv:1708.09723 [hep-ph], accepted for publication in EPJC.
- [13] F. Pisano, V. Pleitez, Phys. Rev. D 46, 410 (1992); P. H. Frampton, Phys. Rev. Lett. 69, 2889 (1992).
- [14] M. Singer, J.W. F. Valle, and J. Schechter, Phys. Rev. D 22, 738 (1980); R. Foot, H. N. Long, and Tuan A. Tran, Phys. Rev. D 50, R34 (1994); J. C. Montero, F. Pisano, and V. Pleitez, Phys. Rev. D 47, 2918 (1993); H. N. Long, Phys. Rev. D 53, 437 (1996); 54, 4691 (1996).
- [15] M.E. Catano, R Martinez, F. Ochoa, Phys.Rev. D86, 073015 (2012); A. G. Dias, C. A. de S.Pires, P. S. Rodrigues da Silva and A. Sampieri, Phys.Rev. D86, 035007 (2012).
- [16] C. Patrignani et al. (Particle Data Group), Chinese Physics C 40, 100001 (2016).
- [17] A. Denner, S. Dittmaier, Nucl.Phys. B734, 62 (2006).
- [18] E. Arganda, M. J. Herrero, X. Marcano and C. Weiland, Phys.Rev. D 91, 015001 (2015); E. Arganda, M.J. Herrero, X. Marcano, R. Morales, A. Szykman, Phys.Rev. D95, 095029 (2017).
- [19] N.H. Thao, L.T. Hue, H.T. Hung, N.T. Xuan, Nucl.Phys. B921, 159 (2017).
- [20] A. Ibarra, E. Molinaro, S.T. Petcov, JHEP 1009, 108 (2010).
- [21] Z. Maki, M. Nakagawa and S. Sakata, Prog. Theor. Phys. 28, 870 (1962); B. Pontecorvo, Sov.Phys.JETP 7, 172 (1958), Zh.Eksp.Teor.Fiz. 34, 247 (1957).
- [22] H. K. Dreiner, H. E. Haber, S. P. Martin, Phys. Rept. **494**, 1 (2010).

- [23] J. A. M. Vermaseren, (2000), arxiv: math-ph/0010025; J. Kuipers, T. Ueda, J. A. M. Vermaseren, and J. Vollinga, Comput. Phys. Commun. 184, 1453 (2013).
- [24] D. Chang, H.N. Long, Phys.Rev. D73, 053006 (2006).
- [25] M. B. Tully and G. C. Joshi, Phys. Rev. D 64, 011301(R) (2001).
- [26] L.T. Hue, L.D. Ninh, Mod.Phys.Lett. A31, 1650062 (2016).
- [27] A.J. Buras, F. D. Fazio, J. Girrbach, M.V. Carlucci, JHEP 1302, 023 (2013).
- [28] H. Okada, N. Okada, Y. Orikasa, K. Yagyu, Phys.Rev. D94, 015002 (2016).
- [29] CMS Collaboration, V. Khachatryan et al., JHEP 1511, 018 (2015).
- [30] A. Denner, S. Heinemeyer, I. Puljak, D. Rebuszi, M. Spira, Eur.Phys.J. C71, 1753 (2011).
- [31] A. J. Buras, F. D. Fazio, J. Girrbach, JHEP 1402, 112 (2014); C. Salazar, R. H. Benavides, W. A. Poncea and E. Rojas, JHEP 1507, 096 (2015).
- [32] G. 't Hooft and M. J. G. Veltman, Nucl. Phys. B44, 189 (1972).
- [33] T. Hahn, M. Perez-Victoria, Comput. Phys. Commun. 118, 153 (1999).
- [34] K.H. Phan, H.T. Hung, and L.T. Hue, Prog. Theor. Exp. Phys.2016, 113B03 (2016).
- [35] J. K. Mizukoshi, C. A. de S. Pires, F. S. Queiroz, P. S. Rodrigues da Silva, Phys. Rev. D 83, 065024 (2011); Alex G. Dias, C. A. de S. Pires and P. S. Rodrigues da Silva, Phys.Lett.B 628, 85 (2005).